

Parameter sensitivity and identifiability for a biogeochemical model of hypoxia in the northern Gulf of Mexico[☆]

Marcus W. Beck*

USEPA National Health and Environmental Effects Research Laboratory, Gulf Ecology Division, 1 Sabine Island Drive, Gulf Breeze, FL 32561

John C. Lehrter

University of South Alabama, Dauphin Island Sea Lab, Dauphin Island, AL 36528

Lisa L. Lowe

CSRA, Inc. supporting the USEPA, Research Triangle Park, NC 27709

Brandon M. Jarvis

USEPA National Health and Environmental Effects Research Laboratory, Gulf Ecology Division, 1 Sabine Island Drive, Gulf Breeze, FL 32561

Abstract

Local sensitivity analyses and identifiable parameter subsets were used to describe numerical constraints of a hypoxia model for bottom waters of the northern Gulf of Mexico. The sensitivity of state variables differed considerably with parameter changes, although most variables were responsive to changes in parameters that influenced planktonic growth rates and less sensitive to physical or chemical parameters. Variation in sensitivity had a direct correspondence with identifiability, such that only small subsets of the complete parameter set had unique effects on the model output. Selecting parameters by decreasing sensitivity demonstrated that only eight of 51 total parameters had a sufficiently unique effect on model output for accurate calibration. As a result, parameter selection heuristics were used

[☆]Version: Tue Aug 15 18:37:33 2017 -0500, [b9430cdc1b195b992ae6ea786f8e485723cf540c](https://doi.org/10.1016/j.ecolmod.2017.08.001)

Acronyms: *chlorophyll a* (chl-*a*); *Coastal General Ecosystem Model* (CGEM); *dissolved oxygen* (O₂); *dissolved organic matter* (DOM); *Gulf of Mexico* (GOM); *Louisiana continental shelf* (LCS); *Mississippi-Atchafalaya River Basin* (MARB); *particulate organic matter* (POM); *root mean squared error* (RMSE); *zero-dimensional* (0-D)

*Corresponding author

Email addresses: beck.marcus@epa.gov (Marcus W. Beck), jlehrter@disl.org (John C. Lehrter), lowe.lisa@epa.gov (Lisa L. Lowe), jarvis.brandon@epa.gov (Brandon M. Jarvis)

to identify parameters for model calibration that depended on combined effects on output, relative sensitivity of each parameter, and ecological categories for the biogeochemical equations. The calibrated zero-dimensional (0-D) unit of the hypoxia model had improved fit to the observed data if sensitive parameters were included in an identifiable subset. Extension of results to a three-dimensional grid of the Gulf of Mexico showed that sensitive parameters for the 0-D model translated to non-trivial changes in the areal estimates of hypoxia.

Keywords: Coastal General Ecosystem Model (CGEM), Gulf of Mexico (GOM), Hypoxia, Identifiability, Sensitivity

1. Introduction

Hypoxia formation in bottom waters of coastal oceans occurs primarily from excess nutrient inputs from land-based sources ([Justić et al., 1987](#); [Diaz and Rosenberg, 1995](#); [Howarth et al., 1996](#)). These events are detrimental to aquatic organisms and have significant negative effects on economic resources derived from coastal ecosystems ([Lipton and Hicks, 2003](#); [Diaz and Rosenberg, 2011](#)). An understanding of the biological, physical, and chemical processes that influence hypoxic areas is a critical concern for mitigating and preventing these negative impacts. Numerical ecosystem models are important tools that synthesize knowledge of ecosystem processes that contribute to hypoxia formation and for predicting the effects of proposed management activities or future scenarios ([Scavia et al., 2004](#); [Hagy and Murrell, 2007](#); [Camacho et al., 2014b](#); [Pauer et al., 2016](#)). Unlike statistical models with more generic structures, simulation and process-based models include explicit descriptions of relevant processes that are constrained by empirical or observational data relevant to the system of interest (e.g. [Omlin et al., 2001b](#); [Eldridge and Roelke, 2010](#)). These models are often coupled with hydrodynamic grids to provide spatially-explicit representations of patterns in

three dimensions (Warner et al., 2005; Dortch et al., 2007; Zhao et al., 2010; Ganju et al., 2016). Combined hydrodynamic and bio-geo-chemical models have been developed specifically to describe hypoxic conditions on the Louisiana continental shelf (LCS) in the northern Gulf of Mexico (GOM) (Fennel et al., 2013; Obenour et al., 2015; Pauer et al., 2016; Lehrter et al., 2017). This area drains a significant portion of the continental United States through the Mississippi-Atchafalaya River Basin (MARB) and is the second largest hypoxic area in the world (Rabalais et al., 2002). Understanding processes that contribute to the frequency and duration of hypoxic events remains a critical research goal for the region.

The development of a model represents a tradeoff between achieving predictive accuracy and a realistic representation of environmental processes. An ideal model is sufficiently generalizable across systems, provides results that are accurate given the inputs, and includes components that are valid descriptions of actual processes (Levins, 1966; Ganju et al., 2016). Given that these characteristics cannot be simultaneously achieved, models are developed that balance predictive accuracy with environmental realism, often favoring one at the expense of the other (Morrison and Morgan, 1999; Ganju et al., 2016). These challenges are analagous to the well-known bias-variance tradeoff in statistical models that balances the competing objectives of over- and under-fitting to an observed dataset. Process-based models are more commonly imbalanced between reality and theory, such that most are over-parameterized in an attempt to completely describe reality (Denman, 2003; Nossent and Bauwens, 2012; Petrucci and Bonhomme, 2014). Quantitative limitations of over-parameterization are analagous to degrees of freedom in standard statistical models as free parameters cannot be numerically estimated when constrained to an observed dataset (Kirchner, 2006). More importantly, over-parameterization can limit use across systems

outside of the data domain and impose uncertainty in model predictions as realistic values for every variable may not be known or inaccurately applied from existing studies (Durand et al., 2002; Refsgaard et al., 2007; Wade et al., 2008).

Model fit can be evaluated relative to the effects of initial conditions or the observed data used for calibration, changes in parameter values, or variation in the structural components (i.e., observational, parameter, or structural uncertainty) (Beck, 1987). Evaluating effects of parameter changes is by far the most common and simplest approach. Although sensitivity analyses should be integrated with model development, parameters are often evaluated post-hoc as a form of ‘damage control’ for further calibration. This approach is sometimes called inverse modelling where results from sensitivity analyses are used to guide calibration or fit of the developed model to observations (Soetaert and Petzoldt 2010, or confronting models with data, *sensu* Hilborn and Mangel 1997). Parameter sensitivity analysis combined with inverse modelling necessarily involves questions of parameter ‘identifiability’. Redundancies in parameter effects lead to unidentifiable models where calibration is empirically impossible (i.e., standard algorithms will not converge) or parameter values may be non-unique leading to the right answer for the wrong reason (Kirchner, 2006). Unidentifiable parameter sets have effects on model output that can be undone or compensated for by alteration of other parameters. Identifiability issues are not foreign to hypoxia or eutrophication models (Omlin et al., 2001a; Estrada and Diaz, 2010; Mateus and Franz, 2015), although there is a clear need for greater integration of these concepts in practice (Fasham et al., 2006).

This study describes a sensitivity and identifiability analysis of a zero-dimensional (0-D) unit of a larger spatial-temporal model of hypoxia dynamics on the LCS. The objectives were to provide a statistical approach that demonstrates numerical limitations of parameter

sets for model calibration and provide a framework for selecting parameters within the identifiability constraints. The specific goals were to 1) identify the parameters that have the greatest influence on state variables using local sensitivity analysis, 2) quantify the identifiability of subsets of the total parameter space based on sensitivity, 3) and provide a set of heuristics for choosing parameters based on sensitivity, identifiability, and parameter categories. The 0-D model was calibrated with selected parameter subsets to demonstrate use of the selection heuristics to improve model fit. Sensitive parameters for the 0-D model were also varied in the larger 3-dimensional model to demonstrate scalability of the results. In addition to dissolved oxygen (O_2), other state variables that were evaluated included ammonium, chlorophyll *a* (chl-*a*), irradiance, nitrate, particulate organic matter (POM), dissolved organic matter (DOM), and phosphorus. In general, we provide empirical results to support the assumption that models are generally over-parameterized and only a finite and smaller subset of the complete parameter set can be optimized.

2. Materials and Methods

2.1. Model description

Hypoxic events, defined as $<2 \text{ mg L}^{-1}$ of O_2 ($< 64 \text{ mmol m}^{-3}$), occur seasonally in bottom waters in the northern GOM. The hypoxic area averages $15,540 \text{ km}^2$ annually (1993-2015) with minimum concentrations observed from late spring to early fall. Seasonal variation is strongly related to carbon and nutrient export from the MARB (Lohrenz et al., 2008; Bianchi et al., 2010), whereas hydrologic variation, currents, and wind patterns can affect vertical salinity gradients that contribute to hypoxia formation (Wiseman et al., 1997; Paerl et al., 1998; Obenour et al., 2015). The Coastal General Ecosystem Model (CGEM) was developed to describe hypoxia dynamics on the LCS and includes elements from the Navy Coastal

Ocean Model ([Martin, 2000](#)) for hydrodynamics and a biogeochemical model with multiple plankton groups, water-column metabolism, and sediment diagenesis ([Eldridge and Roelke, 2010](#)). The hydrodynamic component of CGEM provides a spatially-explicit description of hypoxia using an orthogonal grid with an approximate horizontal resolution of 1.9 km^2 and twenty equally-spaced vertical sigma layers on the shelf. The biogeochemical component includes equations for 36 state variables including six phytoplankton groups (with nitrogen and phosphorus quotas for each), two zooplankton groups, nitrate, ammonium, phosphate, dissolved inorganic carbon, oxygen, silica, and multiple variables for dissolved and particulate organic matter from different sources.

The core unit of CGEM is FishTank, a 0-D model that implements the biogeochemical equations in [Eldridge and Roelke \(2010\)](#) and does not include any advection, mixing, or sediment diagenesis (Fig. 1). A full description of the model structure, equations, and parameters is described in appendices A-F in [Lehrter et al. \(2017\)](#). Although FishTank was developed for specific application in CGEM, it can easily be applied to other hydrodynamic grids. Results are based on time-dependent differential equations that describe energy flow between phytoplankton and zooplankton groups given nutrient uptake rates, organic matter inputs and losses, inherent optical properties, and temperature ([Penta et al. 2008](#); [Eldridge and Roelke 2010](#), see appendices in [Lehrter et al. 2017](#)). A total of 108 equations are estimated at each time step to return values for each of the 36 state variables described by the model. In addition to the initial conditions, 251 parameter values for each of the equations are also supplied at model execution. Values for each of the parameters were based on estimates from the literature, field or laboratory-based measurements, or expert knowledge in absence of the former. As such, a sensitivity analysis of parameter values is

warranted given that, for example, literature or field-based estimates may not apply under all scenarios or expert knowledge is not completely certain (Refsgaard et al., 2007).

The sensitivity of state variables to perturbations of all relevant parameters for the 108 equations was estimated using a five minute timestep with daily output from January 1st to December 31st, 2006. Irrelevant parameters were removed for several reasons; parameters were not relevant for the 0-D model (i.e., hydrodynamic parameters), were considered physical constants, or had no effect given initial conditions. Additionally, FishTank includes six phytoplankton and two zooplankton groups to add complexity in community structure and foodweb dynamics. To remove obvious redundancies, the sensitivity analyses were conducted using only one phytoplankton and one zooplankton group. The final set that was evaluated included 51 parameters that were further grouped into one of six categories based on applicable biogeochemical components of the model: optics ($n = 4$ parameters), organic matter (12), phytoplankton (22), temperature (2), and zooplankton (11) (Table 1). A full description of the model parameters is available as an appendix in Lehrter et al. (2017).

2.2. Local sensitivity analysis

A local sensitivity analysis was performed by evaluating the change in state variables following perturbation of each parameter from its original value (Soetaert and Petzoldt, 2010; Camacho et al., 2014a; RDCT (R Development Core Team), 2017). This approach is described as a First Order Variance Analysis that linearly propagates changes from model parameters to model predictions (Camacho et al., 2014a). Parameters were individually perturbed by a 50% increase of the original values (Table 1) and sensitivity S was estimated for each time step i given a change for parameter j as:

$$S_{ij} = \frac{\partial y_i}{\partial \Theta_j} \cdot \frac{w_{\Theta_j}}{w_{y_i}} \quad (1)$$

where the estimate is based on the change in the predicted value for response variable y divided by the change in the parameter Θ_j multiplied by the quotient of scaling factors w for each. The scaling factors, w_{Θ_j} for the parameter Θ_j and w_{y_i} for response variable y_i , were set as the default value of the unperturbed parameter and the predicted value of y_i after perturbation (Soetaert and Petzoldt, 2010). Scaling makes the estimates unitless to compare model sensitivity to parameters and state variables that differ in relative magnitude. Sensitivity values for all j parameters were summarized as a single value across the time series from $i = 1$ to n as $L1$:

$$L1 = \sum |S_{ij}|/n \quad (2)$$

All parameters for each of the six equation categories (optics, organic matter, phytoplankton, temperature, and zooplankton) that had non-zero $L1$ were retained for identifiability analysis.

2.3. Identifiability and selecting parameter subsets

The collinearity index γ provides a measure of potential redundancies in the response of a state variable to changes in parameter values. The index measures the linear dependence between sensitivity functions (i.e., S_i for j parameters) described above for parameter subsets and was estimated from the minimum eigenvector of the cross-product of a selected sensitivity matrix (Brun et al., 2001; Omlin et al., 2001a):

$$\gamma = \frac{1}{\sqrt{\min(\text{EV}[\hat{S}^\top \hat{S}])}} \quad (3)$$

where γ ranges from one to infinity for perfectly identifiable (orthogonal) or unidentifiable (perfectly collinear) parameter sets. The sensitivity functions were supplied as a matrix \hat{S} with rows i and columns j (eq. (1)) that described deviations of predicted O_2 following perturbations of each parameter. Thus, γ can be estimated from results for any subset of parameter combinations. Sensitivity matrices were first normalized by dividing by the square root of the summed residuals (Omlin et al., 2001a; Soetaert and Petzoldt, 2010). Estimates of γ greater than 10-15 suggest parameter sets are poorly identifiable (Brun et al., 2001; Omlin et al., 2001a), meaning parameter values that maximize fit on a calibration dataset are inestimable by conventional optimization algorithms. An intuitive interpretation of γ is provided by Brun et al. (2001), such that a change in a state variable caused by a change in one parameter can be offset by the fraction $1 - 1/\gamma$ by the remaining parameters. That is, $\gamma = 10$ suggests the relative change in O_2 for an arbitrary parameter in the selected set can be compensated for by 90% with changes in the other parameters.

Parameter selection for model calibration must consider the competing objectives of increased goodness of fit with parameter inclusion and reduced identifiability as it relates to optimization. An additional challenge is a large number of combinations of parameter sets, which complicates selection given sensitivity differences and desired ecological categories of each parameter (e.g., parameters for a group of related structural equations could be of interest). Fig. 2 provides a simple graphic of the unique number of combinations that are possible for different subsets of ‘complete’ parameter sets of different sizes (i.e., n choose k combinations, $n!/(k!(n-k)!)$). The number of unique combinations increases with the

total parameters in the set and is also maximized for moderate selections (e.g., selecting half the total). For example, over 10^{14} combinations are possible by selecting 25 parameters from a set of 50.

A set of heuristics was developed that addresses the tradeoff in model complexity and identifiability given the challenges described above (see also [Wagener et al., 2001](#)). These rulesets were developed to select parameters with preference for those with high sensitivity and identifiability based on $\gamma < 15$ as an acceptable threshold for subsets (e.g., 93% accountability between parameters). Heuristics for parameter selection also recognized that parameter categories (i.e., optics, organic matter, phytoplankton, temperature, zooplankton) may have unequal preferences by users given desired application of the model. For all selection heuristics, parameters were selected by decreasing sensitivity starting with the most sensitive until identifiability did not exceed $\gamma = 15$ where selections were 1) blocked within each of five parameter categories, 2) independent of parameter category, 3) or considering all categories equally.

2.4. Model calibration and scalability

Selected parameter subsets from the seven heuristics were used to calibrate the 0-D model. This analysis demonstrated that different parameter sets can produce model output with differing goodness of fit and calibration effort given 1) differences in variable sensitivity to parameters in each subset, 2) differences in the parameters selected from different categories (heuristic difference), and 3) differences in identifiability values. Generally, this analysis was a proof of concept that the selection heuristics can lead to an ‘optimal’ model by maximizing the balance between sensitivity and identifiability.

Estimates of oxygen production from closed bottle experiments were used to calibrate

the 0-D model. Surface water was collected from a fixed location in Pensacola Bay, Florida () on September 25th, 2013. Water samples were placed into closed 100 mL glass bottles at the time of collection and transported back to the lab for treatments. Concentrations of O₂ and nutrients (NH₄⁺, NO₂⁻, NO₃⁻, PO₄³⁻, and SiO₃²⁻) were extracted from the samples within one hour of collection. Oxygen concentrations were established using Winkler reagents (Parsons et al. 1985) and titration using a MetrOhm Titrand with thiosulfate titrant calibrated against an iodate standard and electrochemical endpoint detection. Ammonium was analyzed using a fluorometric method (Holmes et al. 1999); other nutrients were analyzed using either a Thermo Fisher Aquakem 200 discrete analyzer or an Astoria-Pacific continuous flow analyzer using standard colorimetric methods (APHA 2005).

Oxygen production after an approximate 12 hour period was estimated within the bottles using three treatments: light, dark, and light plus nutrients. All treatments were allowed to sit under ambient outdoor conditions in a water bath with continuous flow at the laboratory. The dark treatments used opaque black bottles to ensure no exposure of ambient light to the samples. The nutrient treatments were supplemented with an equal mix of 25 mmol m⁻³ of ammonium and nitrate and 1.7 mmol m⁻³, approximately two order of magnitude above ambient concentrations. The exposure experiments began at 7am and were concluded at 7pm, after which the concentrations of O₂ in each bottle were measured. Four replicates of each treatment were used. HOBO[®] pendants were used to measure continuous temperature and light for each treatment.

Each parameter subset was calibrated to the ending O₂ concentration for each of the four replicates per treatment. The initial values Parameter values were searched using the optim function in R that implemented the limited memory modification of the BFGS quasi-

Newton method (Byrd et al., 1995; Nocedal and Wright, 2006; RDCT (R Development Core Team), 2017). This optimization scheme searches for values within the user-defined lower and upper bounds of each parameter. We set the algorithm to search within an expected range chosen by the authors to best reflect... While we recognize that ‘actual’ parameter values could possibly extend beyond this range, constraining the values to the range tested herein was expected to produce output that was more interpretable within the context of the sensitivity functions defined above. Moreover, precise limits on each parameter were less of a concern for the current analysis as our primary goal was to demonstrate differences in fit as a function of sensitivity and identifiability. The optimal values for each parameter were identified based on convergence of the model results as a minimization of the root mean squared error (*RMSE*) between the observed and modelled data.

As a final analysis, effects of parameter changes on the larger 3-dimensional model were evaluated to demonstrate that results from the 0-D FishTank model are scalable. For simplicity, only the most sensitive parameter in each category was selected. The CGEM model was run for one year using the default parameter conditions and by increasing each of the selected parameters by 50%. This produced six spatially-referenced time series (one default, five for each parameter change) from which changes in the daily hypoxic area (number of cells < 64 mmol O_2) were estimated.

3. Results

3.1. Local sensitivity analysis

Local sensitivity analyses showed that O_2 was sensitive to perturbations in 38 of the 51 (75% of total) parameters that were evaluated in FishTank (Fig. 3, Table 2). Within each parameter category, O_2 was sensitive to three parameters for optics (75% of all optic

parameters), eight for organic matter (67%), 16 for phytoplankton (73%), one for temperature (50%), and 10 for zooplankton (91%). Although O_2 had the greatest sensitivity to parameters in the zooplankton category (as percentage of total), the relative effects varied. Among all parameters, average sensitivity was $L1 = 9.2 \times 10^{-3}$ with values ranging from $L1 = 8.34 \times 10^{-8}$ for $QminP$ (phytoplankton) to 0.05 for $umax$ (phytoplankton). Within categories (excluding temperature with one sensitive parameter), sensitivity ranged from 4.39×10^{-5} ($astarOMA$) to 7.51×10^{-4} ($astar490$) for optics, 4.17×10^{-4} ($KNH4$) to 6.15×10^{-3} ($KG1$) for organic matter, 8.34×10^{-8} ($QminP$) to 0.05 ($umax$) for phytoplankton, and 3.69×10^{-5} (ZQp) to 0.05 (ZKa) for zooplankton (Table 2). Average sensitivity values in each category were $L1 = 2.81 \times 10^{-4}$ for optics, 2.17×10^{-3} for organic matter, 0.02 for temperature, 0.01 for phytoplankton, and 0.01 for zooplankton.

Local sensitivity analyses for the additional state variables (ammonium, chl-*a*, irradiance, nitrate, POM, DOM, and phosphorus) had similar results as O_2 with some exceptions (Fig. 3 and Tables S1 to S7). All variables were sensitive to the same parameters as O_2 (38 of 51 evaluated), although average sensitivity differed between variables. Average $L1$ ranged from 0.02 for irradiance (Table S3) to 0.71 for DOM (Table S6). All average sensitivity values for the state variables were higher than the average for O_2 ($L1 = 9.2 \times 10^{-3}$). For each variable, $L1$ ranged from 2.24×10^{-6} ($QminP$) to 8.49 (mA) for ammonium (Table S1), 1.38×10^{-6} ($QminP$) to 13.94 (mA) for chl-*a* (Table S2), 1.92×10^{-7} ($QminP$) to 0.13 (ZKa) for irradiance (Table S3), 6.67×10^{-7} ($QminP$) to 8.49 ($umax$) for nitrate (Table S4), 6.41×10^{-5} ($KNH4$) to 7.22 (mA) for POM (Table S5), 7.41×10^{-5} ($KNH4$) to 14.25 (mA) for DOM (Table S6), and 8.21×10^{-7} ($QminP$) to 1.47 (ZKa) for phosphate (Table S7). For the parameter categories, ammonium was most sensitive to phytoplankton parameters

(average $L1 = 0.8$ across all parameters in the category), chl-*a* to phytoplankton ($L1 = 1.14$), irradiance to zooplankton ($L1 = 0.03$), nitrate to zooplankton ($L1 = 1.06$), POM to temperature ($L1 = 0.86$), DOM to temperature ($L1 = 1.48$), and phosphate to zooplankton ($L1 = 0.31$). Finally, average sensitivity between parameter categories independent of the state variables ranged from 8.38×10^{-3} for optics (average $L1$ across all variables) to 0.62 for phytoplankton.

3.2. Identifiability of parameter subsets and selection rules

The identifiability analyses suggested that many parameter subsets exceeded the thresholds of $\gamma = 10, 15$. Parameter identifiability for O_2 decreased (increasing γ) at different rates with increasing size of parameter subsets depending on the parameter category or the number of top parameters that were selected (Fig. 4). By category, identifiability was lowest for all combinations of parameter subsets in the phytoplankton (60% of subsets less than $\gamma = 15$, 43% less than $\gamma = 10$) and zooplankton categories (53.1% less than $\gamma = 15$, 40% less than $\gamma = 10$), whereas all combinations were identifiable for optics (100% less than $\gamma = 15, 10$) and a majority identifiable for organic matter (91.9% less than $\gamma = 15$, 76.5% less than $\gamma = 10$). Identifiability for parameters in the temperature category was not evaluated because O_2 was sensitive to only one parameter (i.e., $\gamma = 1$). Parameter combinations for choosing from the top, top two, top three, and top four parameters in each category together had decreasing identifiability with the increasing size of the selection pool (e.g., top one versus top four parameters, Fig. 4). The percentage of parameter subsets that were below the acceptable thresholds for identifiability was 100% less than $\gamma = 15, 10$ for the top parameter in each category, 90.6% and 80.7% for the top two, 80.7% and 70.9% for the top three, and 55.8% and 45.7% for the top four. Results for the remaining state variables had similar patterns

in identifiability with increasing size of parameter subsets and selection categories, although differences in identifiability between state variables was observed (Fig. 5). Most notably, nitrate was consistently the least identifiable variable (highest overall γ), whereas O_2 was most identifiable.

An evaluation of the effects of individual parameters on γ suggested that some parameters had disproportionate effects on identifiability. Based on $\gamma = 15$, Fig. 4 suggests that most parameter sets for organic matter were identifiable, regardless of how many parameters were selected (i.e., two through eight). However, some subsets were not identifiable such that identification of one or more redundant parameters that are inflating γ values could provide useful information. Fig. 6 shows an alternative view of identifiability of O_2 with exclusion and inclusion of individual parameters in different sets for the organic matter category. As before, collinearity increases with more parameters in a subset, although the increase varies depending on which parameter was included or excluded from the set. For example, inclusion of *KNO3* in a parameter set almost always inflated γ . All parameter subsets that did not include *KNO3* were well below $\gamma = 15$, suggesting that exclusion of this parameter improves identifiability. Interestingly, the inclusion of some parameters caused a reduction in γ , which contradicts the general rule that more parameters caused reduced identifiability. For example, parameter sets that included *KGcdom* generally had lower γ values relative to those that excluded the parameter.

Results for each of the three selection heuristics (blocked by parameter category, independent of category, all categories equally) applied to each state variable differed in the number of selected parameters and distribution of parameters within each category (Tables 3 to 5). In general, a correspondence was observed between the number of parameters that were

selected given the threshold of $\gamma = 15$ and relative identifiability between the state variables. As noted above, nitrate was the least identifiable variable (Fig. 5), whereas other variables (e.g., O_2 , irradiance) were more identifiable. The constraints on identifiability between variables were demonstrated with the selection heuristics. For example, heuristics for nitrate typically selected only one or two parameters that met the criteria as compared to more identifiable variables that included several parameters. Overall, the first selection heuristic demonstrated that the number of parameters chosen by parameter category differed independently of the state variables (Table 3). The number of selected parameters averaged across state variables in decreasing order was 4.25 parameters from the phytoplankton category, 3.5 from organic matter, 2.75 from optics, and 2.38 from zooplankton. The second and third selection heuristics (Tables 4 and 5) were similar, although more parameters were generally selected for the third heuristic given equal importance between categories.

3.3. Model calibration and scalability

Calibration of parameter values for each of the seven selection heuristics (Tables 3 to 5) produced model output that varied in goodness of fit and computational effort required to identify optimal values (Table 6). As expected, the number of required iterations of the optimization algorithm to minimize *RMSE* of observed O_2 and model output varied in proportion to the number of parameters in a subset. For example, only three iterations were required to optimize the single parameter selected for the temperature category, whereas 289 iterations were required for the eight parameters selected independent of category. No association was observed between collinearity (γ) and number of iterations or calibration. Of the seven parameter subsets, selection independent of parameter category and equally within each category produced the largest reduction in *RMSE* values from the default out-

put (starting $RMSE$ 35.33 mmol O₂ m⁻³, reduction to 35.29, 35.32, respectively), whereas the optimal values for parameters in the Optics category had the smallest reduction (35.33). Lower $RMSE$ was associated with higher average sensitivity of a parameter subset. Parameters selected only in the optics category had the highest $RMSE$ and lowest average L1 (2.81×10^{-4} , three parameters), whereas parameters selected independent of category had the lowest $RMSE$ and highest average L1 (0.03, eight parameters, Table 6).

The estimated areal extent of bottom-water hypoxia using default parameter values for the 3-dimensional model peaked on August, 28th at 1.19×10^4 km² (Fig. 8a, August mean area 8988 ± 551 km², Fig. 8b). Increases in the top sensitive parameters for O₂ in each category (Table 2) increased the estimated areal extent of hypoxia (Figs. 8c, 8e), with the exception of the parameter for optimum temperature of growth ($T_{ref}(nospA+nospZ)_{p1}$), which caused a decrease (mean difference from July default area -1070 ± 1161 km², Fig. 8d). The largest increase in area was caused by an increase in the maximum growth rate of phytoplankton ($umax$), with the greatest increase occurring in July (monthly mean increase of 4109 ± 1085 km², Fig. 8d). Overall, changes in hypoxia extent were largest for parameters with large sensitivity values (i.e., L1 = 0.05 for ZKa , L1 = 0.05 for $umax$).

4. Discussion

State variables were most sensitive to phytoplankton and zooplankton parameters, particularly the maximum growth rates ($umax$ for phytoplankton, $Zumax$ for zooplankton), mortality coefficient for phytoplankton (mA), and the zooplankton half saturation coefficient for grazing (ZKa). An increase in the growth rate of primary producers can increase oxygen concentration through photosynthetic processes, although increased production of organic matter is balanced with respiration and bacterial decomposition that reduce O₂ in the water

column. Similarly, increases in zooplankton abundance with increased growth rates can reduce phytoplankton biomass through grazing, which is expected to further deplete pools of organic matter from algal sources. Most variables were also sensitive to variation in the half-saturation grazing coefficient which moderates nutrient concentrations that support half the maximum grazing rate. Although the tradeoff between abundance, grazing, and decomposition is complex, the sensitivity of model state variables to parameters that directly control the abundance of primary producers is in agreement with empirical observations of factors that influence hypoxia dynamics on the LCS ([Fahnenstiel et al., 1995](#); [Roelke, 2000](#); [Eldridge and Roelke, 2010](#)). The sensitivity of the model output to variation in other parameters that relate to physical and chemical properties of the system was of secondary importance. That is, state variables were sensitive to changes in light and temperature parameters, although to a lesser extent than biological parameters. As such, the differing sensitivities of state variables to parameters in each of the categories was not unexpected given ecological relationships that are well understood and described by the model.

A general conclusion from the identifiability analyses is that only limited subsets of parameters were identifiable within the constraints of local sensitivity analyses. These results support previous studies that have suggested similarly small subsets of parameters can be identified using traditional calibration schemes (e.g., [Wheater et al., 1986](#); [Ye et al., 1997](#); [Omlin et al., 2001a](#)). In addition to CGEM, these conclusions have relevance for other biogeochemical models that include numerous parameters and structural equations to characterize processes in the model domain. A general conclusion is that less complex models are potentially beneficial given that only a small subset of parameters is identifiable and that ecosystem processes may in fact be sufficiently characterized with few parameters ([Ye et al.,](#)

1997). Conversely, others have argued that model complexity is not in itself a disadvantage when parsimony is not the only determinant of model structure (Reichert and Omlin, 1997). Over-parameterization can be useful if processes have importance that were not evaluated during model identification. Single objective functions that maximize model fit with identifiable parameters may also provide an incomplete characterization of model worth, which has prompted the development of probability-based models of hypoxia that explicitly include uncertainty in model components (e.g. Obenour et al., 2015). Our results demonstrated that approximately 75% of the evaluated parameters had an effect on the eight state variables, whereas CGEM includes a total of 36 variables and multiple plankton groups, not all of which have immediate concern for understanding hypoxia. The redundancies identified with the sensitivity analyses are challenging only if the primary interest is, for example, O_2 dynamics. Moreover, the proposed selection heuristics provide flexibility for choosing different parameters with the assumption that those chosen depend on the research or management question.

Results from the identifiability analyses provided additional insight into the interactions of parameters in large biogeochemical models. First, identifiability of parameter subsets was not related to the sensitivity of individual variables. As noted above, an identifiable parameter is one that has a unique effect on model predictions that cannot be compensated for or undone by changing other parameters. The magnitude of the effect of a parameter has no bearing on identifiability, which further complicates the selection of parameters for calibration. Although identifiability is the primary limiting factor in choosing a set, the relative sensitivities are more important for the decision to include or exclude individual parameters. For example, Table 6 and Fig. 8 demonstrated that parameter sets with sensitive

parameters had improved model fit and that these parameters had affects that translated to the larger model. Our analysis addressed this challenge by presenting multiple selection criteria for identifiable parameter sets that prioritized the most sensitive parameters during the selection process. Similarly, identifiability was not always related to the number of parameters in a set. Although the general trend was decreasing identifiability with more parameters, the unique effects of including an individual parameter with an existing set often reduced the γ estimate. For example, Fig. 6 showed that including *KGcdom*, *KO2*, or *nitmax* in parameter sets more often reduced γ relative to sets that excluded the parameters. The selection criteria proposed above can facilitate parameter selection and also provide diagnostic tools to identify parameters with disproportionate effects on γ .

4.1. Recommendations and conclusions

Our results demonstrated that small parameter subsets relative to all sensitive parameters were within the identifiability thresholds described in the literature. The identifiable parameter subsets varied considerably between state variables and the method for parameter selection. Use of identifiable parameter subsets with sensitive parameters improved model fit and results for the smaller model were scalable to the 3-dimensional model. However, an evaluation of sensitivity and identifiability of relevant parameter sets is a preliminary and simplistic approach to improving model predictions. We have provided a general approach to select parameter subsets for further model development depending on the ecological context (i.e., selection by parameter category, selection for specific state variables). Thus, the results described above have relevance for model refinement with the specific goal of better understanding ecological dynamics that moderate hypoxia on the northern GOM. The general principles of sensitivity and parameter identifiability have broad applicability beyond this

context and we argue that such methods should be more universally applied as an initial approach to quantify numerical constraints of biogeochemical models.

The effects of structural or observational uncertainty could be evaluated as an extension of the analyses presented above. For example, the sensitivity of O_2 to variation in the half-saturation constants for phytoplankton (the concentration supporting half the maximum uptake rate of nutrients) could vary given the initial nutrient concentrations (Eppley et al., 1969). Further, changes in the ratio between nitrogen and phosphorus could affect the sensitivity of state variables to parameter changes depending on the limiting nutrient. A more challenging analysis is an evaluation of the effects of structural components on model output, which requires exclusion or inclusion of explicit biogeochemical equations. The FishTank model includes several ‘switches’ that allow users to change the governing equations that estimate state variables, such as switches that ‘turn on’ different structural equations for light attenuation in the water column. This design is uncommon in biogeochemical models and could be leveraged for an evaluation of structural uncertainty. As such, our analysis of parameter sensitivity and identifiability could be combined with an evaluation of observational and structural uncertainty for a more complete characterization of the model, having implications for understanding drivers of hypoxia in coastal waters.

Acknowledgments

We thank the research staff of the USEPA Gulf Ecology Division, Environmental Modeling and Visualization Laboratory, and Naval Research Laboratory for their efforts developing the hydrodynamic and biogeochemical components of CGEM. We thank James Pauer, Yonghsan Wan, and Susan Elizabeth George for providing helpful comments on an earlier draft.

Role of Funding Sources

This study was funded, reviewed, and approved for publication by the US EPA, National Health and Environmental Effects Research Laboratory. However, the views expressed in this paper are those of the authors and do not necessarily reflect the views or policies of the US EPA.

- Beck, M. B., 1987. Water quality modeling: A review of the analysis of uncertainty. *Water Resour. Res.* 23 (8), 1393–1442.
- Beck, M. W., Hagy III, J. D., Murrell, M. C., 2015. Improving estimates of ecosystem metabolism by reducing effects of tidal advection on dissolved oxygen time series. *Limnol. Oceanogr. Methods* 13 (12), 731–745.
- Bianchi, T. S., DiMarco, S. F., Jr, J. H. C., Hetland, R. D., Chapman, P., Day, J. W., Allison, M. A., 2010. The science of hypoxia in the Northern Gulf of Mexico: a review. *Sci. Total. Environ.* 408 (7), 1471–1484.
- Brun, R., Reichert, P., Künsch, H. R., 2001. Practical identifiability analysis of large environmental simulation models. *Water Resour. Res.* 37 (4), 1015–1030.
- Byrd, R. H., Lu, P., Nocedal, J., Zhu, C., 1995. A limited memory algorithm for bound constrained optimization. *SIAM J. Sci. Comput.* 16 (5), 1190–1208.
- Camacho, R. A., Martin, J. L., Diaz-Ramirez, J., McAnally, W., Rodriguez, H., Suscy, P., Zhang, S., 2014a. Uncertainty analysis of estuarine hydrodynamic models: an evaluation of input data uncertainty in the Weeks Bay estuary, Alabama. *Appl. Ocean. Res.* 47, 138–153.
- Camacho, R. A., Martin, J. L., Watson, B., Paul, M. J., Zheng, L., Stribling, J. B., 2014b. Modeling the factors controlling phytoplankton in the St. Louis Bay estuary, Mississippi and evaluating estuarine responses to nutrient load modifications. *J. Environ. Eng.* 141 (3), 04014067.
- Denman, K. L., 2003. Modelling planktonic ecosystems: parameterizing complexity. *Prog. Oceanogr.* 57 (3-4), 429–452.

- Diaz, R. J., Rosenberg, R., 1995. Marine benthic hypoxia: A review of its ecological effects and the behavioural responses of benthic macrofauna. *Oceanogr. Mar. Biology* 33, 245–303.
- Diaz, R. J., Rosenberg, R., 2011. Introduction to environmental and economic consequences of hypoxia. *Int. J. Water Resour. Dev.* 27 (1), 71–82.
- Dortch, M. S., Zakikhani, M., Noel, M. R., Kim, S. C., 2007. Application of a water quality model to Mississippi Sound to evaluate impacts of freshwater diversions. Tech. rep., Engineer Research and Development Center, Vicksburg, Mississippi.
- Durand, P., Gascuel-Oudou, C., Cordier, M. O., 2002. Parameterisation of hydrological models: a review and lessons learned from studies of an agricultural catchment (Naisin, France. *Agron.* 22 (2), 217–228.
- Eldridge, P. M., Roelke, D. L., 2010. Origins and scales of hypoxia on the Louisiana shelf: importance of seasonal plankton dynamics and river nutrients and discharge. *Ecol. Model.* 221 (7), 1028–1042.
- Eppley, R. W., Rogers, J. N., McCarthy, J., 1969. Half-saturation constants for uptake of nitrate and ammonium by marine phytoplankton. *Limnol. Oceanogr.* 14 (6), 912–920.
- Estrada, V., Diaz, M., 2010. Global sensitivity analysis in the development of first principle-based eutrophication models. *Environ. Model. Softw.* 25, 1539–1551.
- Fahnenstiel, G. L., McCormick, M. J., Lang, G. A., Redalje, D. G., Lohrenz, S. E., Markowitz, M., Wagoner, B., Carrick, H. J., 1995. Taxon-specific growth and loss rates for dominant phytoplankton populations from the northern Gulf of Mexico. *Mar. Ecol. Prog. Ser.* 117 (1-3), 229–239.

- Fasham, M. J. R., Flynn, K. J., Pondaven, P., Anderson, T. R., Boyd, P. W., 2006. Development of a robust marine ecosystem model to predict the role of iron in biogeochemical cycles: A comparison of results for iron-replete and iron-limited areas, and the SOIREE iron-enrichment experiment. *Deep. Res. I* 53, 333–366.
- Fennel, K., Hu, J., Laurent, A., Marta-Almeida, M., Hetland, R., 2013. Sensitivity of hypoxia predictions for the northern Gulf of Mexico to sediment oxygen consumption and model nesting. *J. Geophys. Res. Ocean.* 118 (2), 990–1002.
- Ganju, N. K., Brush, M. J., Rashleigh, B., Aretxabaleta, A. L., del Barrio, P., Grear, J. S., Harris, L. A., Lake, S. J., McCardell, G., O'Donnell, J., Ralston, D. K., Signell, R. P., Testa, J. M., Vaudrey, J. M. P., 2016. Progress and challenges in coupled hydrodynamic-ecological estuarine modeling. *Estuaries Coasts* 39 (2), 311–332.
- Hagy, J. D., Murrell, M. C., 2007. Susceptibility of a northern Gulf of Mexico estuary to hypoxia: An analysis using box models. *Estuar. Coast. Shelf Sci.* 74, 239–253.
- Hilborn, R., Mangel, M., 1997. *The Ecological Detective: Confronting Models with Data*. Princeton University Press, Princeton, New Jersey.
- Howarth, R. W., Billen, G., Swaney, D., Townsend, A., Jaworski, N., Lajtha, K., Downing, J. A., Elmgren, R., Caraco, N., Jordan, T., Berendse, F., Freney, J., Kudeyarov, V., Murdoch, P., Zhao-Liang, Z., 1996. Regional nitrogen budgets and riverine N & P fluxes for the drainages to the North Atlantic Ocean: natural and human influences. *Biogeochem.* 35 (1), 75–139.
- Justić, D., Legović, T., Rottini-Sandrini, L., 1987. Trends in oxygen content 1911–1984 and

- occurrence of benthic mortality in the northern Adriatic Sea. *Estuar. Coast. Shelf Sci.* 25 (4), 435–445.
- Kirchner, J. W., 2006. Getting the right answers for the right reasons: Linking measurements, analyses, and models to advance the science of hydrology. *Water Resour. Res.* 42 (3), W03S04.
- Lehrter, J. C., Ko, D. S., Lowe, L. L., Penta, B., 2017. Predicted effects of climate change on northern Gulf of Mexico hypoxia. In: Justic et al. (Ed.), *Modeling Coastal Hypoxia: Numerical Simulations of Patterns, Controls, and Effect of Dissolved Oxygen Dynamics*. Springer, New York, pp. 173–204.
- Levins, R., 1966. The strategy of model building in population biology. *Am. Sci.* 54 (4), 421–431.
- Lipton, D., Hicks, R., 2003. The cost of stress: low dissolved oxygen and economic benefits of recreational striped bass (*Morone saxatilis*) fishing in the Patuxent River. *Estuaries* 26 (2A), 310–315.
- Lohrenz, S. E., Redalje, D. G., Cai, W. J., Acker, J., Dagg, M., 2008. A retrospective analysis of nutrients and phytoplankton productivity in the Mississippi River plume. *Cont. Shelf Res.* 28 (12), 1466–1475.
- Martin, P. J., 2000. Description of the navy coastal ocean model version 1.0. Tech. Rep. NRL/FR/7322-00-9962, Naval Research Lab, Stennis Space Center, Mississippi.
- Mateus, M. D., Franz, G., 2015. Sensitivity analysis in a complex marine ecological model. *Water* 7, 2060–2081.

- Morrison, M., Morgan, M. S., 1999. Models as mediating agents. In: Morgan, M. S., Morrison, M. (Eds.), *Models as Mediators*. Cambridge University Press, Cambridge, p. 401.
- Nocedal, J., Wright, S. J., 2006. *Numerical Optimization*, 2nd Edition. Springer-Verlag, New York, New York.
- Nossent, J., Bauwens, W., 2012. Multi-variable sensitivity and identifiability analysis for a complex environmental model in view of integrated water quantity and water quality modeling. *Water Sci. Technol.* 65 (3), 539–549.
- Obenour, D. R., Michalak, A. M., Scavia, D., 2015. Assessing biophysical controls on Gulf of Mexico hypoxia through probabilistic modeling. *Ecol. Appl.* 25 (2), 492–505.
- Omlin, M., Brun, R., Reichert, P., 2001a. Biogeochemical model of Lake Zürich: sensitivity, identifiability and uncertainty analysis. *Ecol. Model.* 141 (1-3), 105–123.
- Omlin, M., Reichert, P., Forster, R., 2001b. Biogeochemical model of Lake Zürich: model equations and results. *Ecol. Model.* 141 (1-3), 77–103.
- Paerl, H. W., Pinckney, J. L., Fear, J. M., Peierls, B. L., 1998. Ecosystem responses to internal and watershed organic matter loading: consequences for hypoxia in the eutrophying Neuse River Estuary, North Carolina, USA. *Mar. Ecol. Prog. Ser.* 166, 17–25.
- Pauer, J. J., Feist, T. J., Anstead, A. M., DePetro, P. A., Melendez, W., Lehrter, J. C., Murrell, M. C., Zhang, X., Ko, D. S., 2016. A modeling study examining the impact of nutrient boundaries on primary production on the Louisiana continental shelf. *Ecol. Model.* 328, 136–147.
- Penta, B., Lee, Z., Kudela, R. M., Palacios, S. L., Gray, D. J., Jolliff, J. K., Shulman, I. G.,

2008. An underwater light attenuation scheme for marine ecosystem models. *Opt. Express* 16 (21), 16581–16591.
- Petrucci, G., Bonhomme, C., 2014. The dilemma of spatial representation for urban hydrology semi-distributed modelling: trade-offs among complexity, calibration and geographical data. *J. Hydrol.* 517, 997–1007.
- Rabalais, N. N., Turner, R. E., Scavia, D., 2002. Beyond science into policy: Gulf of Mexico hypoxia and the Mississippi river. *Biosci.* 52 (2), 129–142.
- RDCT (R Development Core Team), 2017. R: A language and environment for statistical computing, v3.3.2. R Foundation for Statistical Computing, Vienna, Austria. <http://www.R-project.org>.
- Refsgaard, J. C., van der Sluijs, J. P., Højberg, A. L., Vanrolleghem, P. A., 2007. Uncertainty in the environmental modelling process - a framework and guidance. *Environ. Model. Softw.* 22 (11), 1543–1556.
- Reichert, P., Omlin, M., 1997. On the usefulness of over parameterized ecological models. *Ecol. Model.* 95 (2), 289–299.
- Roelke, D. L., 2000. Copepod food-quality threshold as a mechanism influencing phytoplankton succession and accumulation of biomass, and secondary productivity: a modeling study with management implications. *Ecol. Model.* 134, 245–274.
- Scavia, D., Justic, D., Bierman, V. J., 2004. Reducing hypoxia in the Gulf of Mexico: Advice from three models. *Estuaries* 27 (3), 419–425.
- Soetaert, K., Petzoldt, T., 2010. Inverse modelling, sensitivity, and Monte Carlo analysis in R using package FME. *J. Stat. Softw.* 33 (3), 1–28.

- Wade, A. J., Jackson, B. M., Butterfield, D., 2008. Over-parameterised, uncertain ‘mathematical marionettes’ - how can we best use catchment water quality models? An example of an 80-year catchment-scale nutrient balance. *Sci. Total. Environ.* 400 (1-3), 52–74.
- Wagener, T., Boyle, D. P., Lees, M. J., Wheater, H. S., Gupta, H. V., Sorooshian, S., 2001. A framework for development and application of hydrological models. *Hydrol. Earth Syst. Sci.* 5 (1), 13–26.
- Warner, J. C., Geyer, W. R., Lerczak, J. A., 2005. Numerical modeling of an estuary: a comprehensive skill assessment. *J. Geophys. Res. Ocean.* 110 (C5), 13.
- Wenner, E., Sanger, D., Arendt, M., Holland, A. F., Chen, Y., 2004. Variability in dissolved oxygen and other water-quality variables within the National Estuarine Research Reserve System. *J. Coast. Res.* 45 (SI), 17–38.
- Wheater, H. S., Bishop, K. H., Beck, M. B., 1986. The identification of conceptual hydrological models for surface water acidification. *Hydrol. Process.* 1 (1), 89–109.
- Wiseman, W. J., Rabalais, N. N., Turner, R. E., Dinnel, S. P., MacNaughton, A., 1997. Seasonal and interannual variability within the Louisiana coastal current: stratification and hypoxia. *J. Mar. Syst.* 12 (1-4), 237–248.
- Ye, W., Bates, B. C., Viney, N. R., Sivapalan, M., Jakeman, A. J., 1997. Performance of conceptual rainfall-runoff models in low yielding ephemeral catchments. *Water Resour. Res.* 33 (1), 153–166.
- Zhao, L., Chen, C., Vallino, J., Hopkinson, C., Beardsley, R. C., Lin, H., Lerczak, J., 2010. Wetland-estuarine-shelf interactions on the Plum Island Sound and Merrimack River in the Massachusetts coast. *J. Geophys. Res.* 115 (C10), 13.

Table 1: FishTank parameters evaluated for sensitivity and identifiability. Sensitivity analyses were based on a 50% increase (Value \cdot 1.5) from the initial value of each parameter. Dashed units are dimensionless. Parameters are grouped by categories as optics, temperature, phytoplankton, zooplankton, and organic matter. A full description of the model structure, equations, and parameters is described in [Lehrter et al. \(2017\)](#).

Description	Parameter	Units	Value	Value \cdot 1.5
Optics				
Chla specific absorption at 490 nm	<i>astar490</i>	$\text{m}^{-1} (\text{mg Chla m}^{-3})^{-1}$	0.04	0.06
OMA specific absorption at 490 nm	<i>astarOMA</i>	$\text{m}^{-1} (\text{mg OMA m}^{-3})^{-1}$	0.1	0.15
OMZ specific absorption at 490 nm	<i>astarOMZ</i>	$\text{m}^{-1} (\text{mg OMZ m}^{-3})^{-1}$	0.1	0.15
sinking rate	<i>sink CDOM</i>	m d^{-1}	0	0
Temperature				
Optimum temperature for growth	<i>Tref(nospA+nospZ)_{p1}</i>	C	22	33
Optimum temperature for growth	<i>Tref(nospA+nospZ)_{p1}</i>	C	22	33
Phytoplankton				
initial slope of photosynthesis v irradiance	<i>alpha</i>	$10^{-16} \text{ cm}^2 \text{ s quanta}^{-1} \text{ d}^{-1}$	8.42×10^{-17}	1.26×10^{-16}
coefficient for non-limiting nutrient	<i>aN</i>	-	1	1.5
phytoplankton threshold for grazing	<i>Athresh</i>	$10^7 \text{ cells m}^{-3}$	1.72×10^8	2.58×10^8
edibility vector for Z1	<i>ediblevector(Z1)</i>	-	0.25	0.38
edibility vector for Z2	<i>ediblevector(Z2)</i>	-	0.25	0.38
half-saturation constant for N	<i>Kn</i>	mmol m^{-3}	4.51	6.76
half-saturation constant for P	<i>Kp</i>	mmol m^{-3}	2.86	4.29
Qn constant for Flynn growth model	<i>KQn</i>	-	5	7.5
Qp constant for Flynn growth model	<i>KQp</i>	-	0.2	0.3
half-saturation constant for Si uptake	<i>Ksi</i>	mmol m^{-3}	4.51	6.76
mortality coefficient	<i>mA</i>	d^{-1}	0.1	0.15
phytoplankton carbon/cell	<i>Qc</i>	$10^{-7} \text{ mmol C cell}^{-1}$	1.35×10^{-6}	2.03×10^{-6}
minimum N cell-quota	<i>QminN</i>	$10^{-9} \text{ mmol N cell}^{-1}$	6.08×10^{-9}	9.12×10^{-9}
minimum P cell-quota	<i>QminP</i>	$10^{-9} \text{ mmol P cell}^{-1}$	6.19×10^{-10}	9.29×10^{-10}
phytoplankton basal respiration coefficient	<i>respb</i>	d^{-1}	0.02	0.03
phytoplankton growth respiration coefficient	<i>respg</i>	-	0.1	0.15
sinking rate of phytoplankton cells	<i>sink A</i>	m d^{-1}	1.49	2.23
maximum growth rate	<i>umax</i>	d^{-1}	0.41	0.62
N-uptake rate measured at umax	<i>vmaxN</i>	$10^{-8} \text{ mmol cell}^{-1} \text{ d}^{-1}$	4.1×10^{-8}	6.15×10^{-8}
P-uptake rate measured at umax	<i>vmaxP</i>	$10^{-8} \text{ mmol cell}^{-1} \text{ d}^{-1}$	2.68×10^{-8}	4.02×10^{-8}
Si-uptake rate measured at umax	<i>vmaxSi</i>	$10^{-8} \text{ mmol cell}^{-1} \text{ d}^{-1}$	4.1×10^{-8}	6.15×10^{-8}
phytoplankton volume/cell	<i>volcell</i>	μm^3	3.37×10^4	5.05×10^4
Zooplankton				
assimilation efficiency as a fraction of ingestion	<i>Zeffic</i>	-	0.4	0.6
half saturation coefficient for grazing	<i>ZKa</i>	$\mu\text{m}^3 \text{ m}^{-3}$	1.12×10^{12}	1.68×10^{12}
quadratic mortality constant	<i>Zm</i>	$\text{m}^6 \text{ ind}^{-2} \text{ d}^{-1}$	7.2×10^{-4}	0
zooplankton carbon/individual	<i>ZQc</i>	mmol C ind^{-1}	3.13×10^{-4}	4.7×10^{-4}
zooplankton nitrogen/individual	<i>ZQn</i>	mmol N ind^{-1}	6.95×10^{-5}	1.04×10^{-4}
zooplankton phosphorus/individual	<i>ZQp</i>	mmol P ind^{-1}	3.77×10^{-6}	5.66×10^{-6}
zooplankton biomass-dependent respiration factor	<i>Zrespb</i>	d^{-1}	0.1	0.15
zooplankton growth-dependent respiration factor	<i>Zrespg</i>	-	0.2	0.3
proportion of phytoplankton lost to sloppy feeding	<i>Zslop</i>	-	0.25	0.38
maximum growth rate of zooplankton	<i>Zumax</i>	$\mu\text{m}^3 \text{ ind}^{-1} \text{ d}^{-1}$	9.45×10^7	1.42×10^8
zooplankton volume/individual	<i>Zvolcell</i>	$\mu\text{m}^3 \text{ ind}^{-1}$	2.98×10^7	4.47×10^7
Organic Matter				
turnover rate for OM1A and OM1Z	<i>KG1</i>	y^{-1}	50	75
turnover rate for OM2A and OM2Z	<i>KG2</i>	y^{-1}	50	75
decay rate of CDOM	<i>KGcdom</i>	d^{-1}	0.01	0.02
NH4 rate constant for nitrification	<i>KNH4</i>	mmol m^{-3}	1	1.5
half-saturation concentration for denitrification	<i>KNO3</i>	mmol m^{-3}	10	15
half-saturation concentration for O2 utilization	<i>KO2</i>	mmol m^{-3}	10	15
O2 concentration that inhibits denitrification	<i>KstarO2</i>	mmol m^{-3}	10	15
maximum rate of nitrification per day	<i>nitmax</i>	$\text{mmol m}^{-3} \text{ d}^{-1}$	0.52	0.78
phytoplankton sinking rate	<i>sink OM1_A</i>	m d^{-1}	10	15
zooplankton sinking rate	<i>sink OM1_Z</i>	m d^{-1}	10	15
phytoplankton sinking rate	<i>sink OM2_A</i>	m d^{-1}	0	0
zooplankton sinking rate	<i>sink OM2_Z</i>	m d^{-1}	0	0

Table 2: Sensitivity of O_2 to perturbations of individual parameters. Sensitivities are based on a 50% increase from the initial parameter value, where $L1$ summarizes differences in model output (see eq. (2)). Parameters that did not affect O_2 are not shown. Parameters are grouped by categories as optics, temperature, phytoplankton, zooplankton, and organic matter.

Description	Parameter	L1
Optics		
Chla specific absorption at 490 nm	<i>astar490</i>	7.51×10^{-4}
OMZ specific absorption at 490 nm	<i>astarOMZ</i>	4.92×10^{-5}
OMA specific absorption at 490 nm	<i>astarOMA</i>	4.39×10^{-5}
Organic Matter		
turnover rate for OM1A and OM1Z	<i>KG1</i>	6.15×10^{-3}
turnover rate for OM2A and OM2Z	<i>KG2</i>	3.14×10^{-3}
O2 concentration that inhibits denitrification	<i>KstarO2</i>	3.04×10^{-3}
decay rate of CDOM	<i>KGcdom</i>	2.98×10^{-3}
half-saturation concentration for O2 utilization	<i>KO2</i>	5.85×10^{-4}
half-saturation concentration for denitrification	<i>KNO3</i>	5.8×10^{-4}
maximum rate of nitrification per day	<i>nitmax</i>	4.99×10^{-4}
NH4 rate constant for nitrification	<i>KNH4</i>	4.17×10^{-4}
Phytoplankton		
maximum growth rate	<i>umax</i>	0.05
mortality coefficient	<i>mA</i>	0.02
initial slope of photosynthesis v irradiance	<i>alpha</i>	0.02
edibility vector for Z1	<i>ediblevector(Z1)</i>	0.02
phytoplankton carbon/cell	<i>Qc</i>	0.01
phytoplankton growth respiration coefficient	<i>respg</i>	8.36×10^{-3}
N-uptake rate measured at umax	<i>vmaxN</i>	8.12×10^{-3}
phytoplankton basal respiration coefficient	<i>respb</i>	6.94×10^{-3}
phytoplankton threshold for grazing	<i>Athresh</i>	4.57×10^{-3}
minimum N cell-quota	<i>QminN</i>	4.32×10^{-3}
P-uptake rate measured at umax	<i>vmaxP</i>	4.27×10^{-3}
coefficient for non-limiting nutrient	<i>aN</i>	4.23×10^{-3}
phytoplankton volume/cell	<i>volcell</i>	4.13×10^{-3}
half-saturation constant for P	<i>Kp</i>	2.9×10^{-3}
half-saturation constant for N	<i>Kn</i>	2.77×10^{-4}
minimum P cell-quota	<i>QminP</i>	8.34×10^{-8}
Temperature		
Optimum temperature for growth	<i>Tref(nospA+nospZ)_{p1}</i>	0.02
Zooplankton		
half saturation coefficient for grazing	<i>ZKa</i>	0.05
zooplankton nitrogen/individual	<i>ZQn</i>	0.02
quadratic mortality constant	<i>Zm</i>	0.02
maximum growth rate of zooplankton	<i>Zumax</i>	0.02
assimilation efficiency as a fraction of ingestion	<i>Zeffic</i>	0.01
proportion of phytoplankton lost to sloppy feeding	<i>Zslop</i>	7.78×10^{-3}
zooplankton growth-dependent respiration factor	<i>Zrespg</i>	5.32×10^{-3}
zooplankton biomass-dependent respiration factor	<i>Zrespb</i>	2.96×10^{-3}
zooplankton carbon/individual	<i>ZQc</i>	9.38×10^{-5}
zooplankton phosphorus/individual	<i>ZQp</i>	3.69×10^{-5}

*Temperature parameters apply separately to phytoplankton ($p1$, one group) or zooplankton ($z1$, one group), denoted by subscripts

Table 3: Parameter identifiability (as γ , eq. (3)) by category for relevant state variables. Selections followed the first heuristic where parameters were selected within categories from most to least sensitive until $\gamma > 15$. Rank describes the relative parameter sensitivity in each category for each state variable. Duplicate parameters and ranks in the first two columns apply only to γ values in the same row (i.e., parameter ranks vary for each variable).

Parameter	Rank	Ammonium	Chl- <i>a</i>	O ₂	Irradiance	Nitrate	POM	DOM	Phosphate
Optics									
<i>astar490</i>	1	1	1	1	1	1	1	1	1
<i>astarOMA</i>	2	7.33	5.42	-	5.36	-	7.78	7.87	-
<i>astarOMZ</i>	2	-	-	1.39	-	-	-	-	4.73
<i>astarOMA</i>	3	-	-	3.87	-	-	-	-	10.04
<i>astarOMZ</i>	3	7.58	5.51	-	6.02	-	7.91	7.87	-
Organic Matter									
<i>KG1</i>	1	-	-	1	-	-	1	-	1
<i>KG2</i>	1	-	-	-	-	-	-	1	-
<i>KGcdom</i>	1	-	1	-	1	-	-	-	-
<i>KstarO2</i>	1	-	-	-	-	1	-	-	-
<i>nitmax</i>	1	1	-	-	-	-	-	-	-
<i>KG1</i>	2	-	1.12	-	1.93	-	-	-	-
<i>KG2</i>	2	-	-	6	-	-	-	-	13.43
<i>KGcdom</i>	2	-	-	-	-	-	1.47	1.39	-
<i>KNH₄</i>	2	4.03	-	-	-	-	-	-	-
<i>KG1</i>	3	4.09	-	-	-	-	-	-	-
<i>KG2</i>	3	-	-	-	8.19	-	-	-	-
<i>KGcdom</i>	3	-	-	-	-	-	-	-	13.75
<i>KO2</i>	3	-	-	-	-	-	14.07	11.96	-
<i>KstarO2</i>	3	-	-	6.04	-	-	-	-	-
<i>KGcdom</i>	4	4.19	-	6.12	-	-	-	-	-
<i>KO2</i>	4	-	-	-	-	-	-	-	14.68
<i>KstarO2</i>	4	-	-	-	10.65	-	14.08	-	-
<i>KO2</i>	5	9.47	-	8.61	-	-	-	-	-
Phytoplankton									
<i>mA</i>	1	1	1	-	-	-	1	1	-
<i>umax</i>	1	-	-	1	1	1	-	-	1
<i>ediblevector(Z1)</i>	2	1.13	1.17	-	-	-	1.15	-	-
<i>mA</i>	2	-	-	1.19	1.29	-	-	-	-
<i>Qc</i>	2	-	-	-	-	11.57	-	-	-
<i>umax</i>	2	-	-	-	-	-	-	1.21	-
<i>vmaxP</i>	2	-	-	-	-	-	-	-	7.45
<i>alpha</i>	3	-	-	1.44	1.98	-	-	-	-
<i>ediblevector(Z1)</i>	3	-	-	-	-	-	-	2.9	-
<i>umax</i>	3	2.73	2.11	-	-	-	3.26	-	-
<i>alpha</i>	4	3.55	4.57	-	-	-	-	-	-
<i>ediblevector(Z1)</i>	4	-	-	2.09	4.09	-	-	-	-
<i>Qc</i>	4	-	-	-	-	-	4.98	-	-
<i>vmaxN</i>	4	-	-	-	-	-	-	4.9	-
<i>alpha</i>	5	-	-	-	-	-	10.11	-	-
<i>Qc</i>	5	-	-	2.9	-	-	-	-	-
<i>vmaxN</i>	5	8.14	-	-	-	-	-	-	-
<i>Athresh</i>	6	11.27	-	-	-	-	-	-	-
<i>respg</i>	6	-	-	3.41	-	-	-	-	-
<i>vmaxN</i>	7	-	-	3.97	-	-	-	-	-
Zooplankton									
<i>ZKa</i>	1	-	-	1	1	1	-	-	1
<i>Zumax</i>	1	1	1	-	-	-	1	1	-
<i>ZKa</i>	2	-	4.31	-	-	-	7.3	5.43	-
<i>ZQn</i>	2	-	-	3.18	6.32	9.76	-	-	8.54
<i>Zm</i>	3	-	-	4.57	-	-	-	-	-
<i>Zumax</i>	3	-	-	-	6.93	-	-	-	-
<i>Zm</i>	4	-	-	-	11.86	-	-	-	-
<i>Zumax</i>	4	-	-	5.2	-	-	-	-	-

Table 4: Parameter identifiability (as γ , eq. (3)) for relevant state variables. Selections followed the second heuristic where parameters were selected independent of category from most to least sensitive (L1, eq. (2)), until $\gamma > 15$. Rank describes the relative parameter sensitivity in each category for each state variable (O: optics, OM: organic matter, P: phytoplankton, T: temperature, Z: zooplankton).

Selections by state variable	Parameter	L1	Rank	γ
Ammonium				
1	mA	8.49	1 _P	1
2	$nitmax$	1.54	1 _{OM}	1.16
3	$Zumax$	1.42	1 _Z	2.9
Chlorophyll				
1	mA	13.94	1 _P	1
2	$Zumax$	1.02	1 _Z	1.18
Dissolved Oxygen				
1	$umax$	0.05	1 _P	1
2	ZKa	0.05	1 _Z	2.17
3	mA	0.02	2 _P	2.31
4	$Tref(nospA+nospZ)_{p1}$	0.02	1 _T	2.37
5	ZQn	0.02	2 _Z	4.69
6	$alpha$	0.02	3 _P	4.91
7	Zm	0.02	3 _Z	6.73
8	$Zumax$	0.02	4 _Z	6.81
DOM				
1	mA	14.25	1 _P	1
2	$Tref(nospA+nospZ)_{p1}$	1.48	1 _T	1.05
3	$umax$	1.11	2 _P	2.46
4	$Zumax$	1.01	1 _Z	2.91
Irradiance				
1	ZKa	0.13	1 _Z	1
2	$umax$	0.09	1 _P	4.41
3	ZQn	0.06	2 _Z	7.54
4	mA	0.05	2 _P	8.17
5	$KGcdom$	0.05	1 _{OM}	9.44
6	$alpha$	0.04	3 _P	9.66
7	$Zumax$	0.04	3 _Z	10.79
Nitrate				
1	$umax$	8.49	1 _P	1
Phosphate				
1	ZKa	1.47	1 _Z	1
2	$umax$	0.78	1 _P	11.45
3	$vmaxP$	0.59	2 _P	11.48
4	ZQn	0.5	2 _Z	13.74
POM				
1	mA	7.22	1 _P	1
2	$Zumax$	0.96	1 _Z	1.15
3	$KG1$	0.92	1 _{OM}	3.87

Table 5: Parameter identifiability (as γ , eq. (3)) for relevant state variables. Selections followed the third heuristic where parameters were selected equally within each category from most to least sensitive (L1, eq. (2)), until $\gamma > 15$. Rank describes the relative parameter sensitivity in each category for each state variable (O: optics, OM: organic matter, P: phytoplankton, T: temperature, Z: zooplankton).

Selections by state variable	Parameter	L1	Rank	γ
Ammonium				
1	mA	8.49	1 _P	1
2	$nitmax$	1.54	1 _{OM}	1.16
3	$Zumax$	1.42	1 _Z	2.9
4	$Tref(nospA+nospZ)_{p1}$	0.79	1 _T	3.46
5	$astar490$	0.03	1 _O	4.25
Chlorophyll				
1	mA	13.94	1 _P	1
2	$Zumax$	1.02	1 _Z	1.18
3	$Tref(nospA+nospZ)_{p1}$	0.6	1 _T	2.62
4	$KGcdom$	0.07	1 _{OM}	3.24
5	$astar490$	0.02	1 _O	5.98
Dissolved Oxygen				
1	$umax$	0.05	1 _P	1
2	ZKa	0.05	1 _Z	2.17
3	$Tref(nospA+nospZ)_{p1}$	0.02	1 _T	2.29
4	$KG1$	6.15×10^{-3}	1 _{OM}	3.85
5	$astar490$	7.51×10^{-4}	1 _O	3.89
6	mA	0.02	2 _P	4.42
7	ZQn	0.02	2 _Z	5.22
DOM				
1	mA	14.25	1 _P	1
2	$Tref(nospA+nospZ)_{p1}$	1.48	1 _T	1.05
3	$Zumax$	1.01	1 _Z	2.61
4	$KG2$	0.94	1 _{OM}	3.39
5	$astar490$	0.04	1 _O	4.46
6	$umax$	1.11	2 _P	6.02
7	ZKa	0.88	2 _Z	9.21
Irradiance				
1	ZKa	0.13	1 _Z	1
2	$umax$	0.09	1 _P	4.41
3	$KGcdom$	0.05	1 _{OM}	4.5
4	$Tref(nospA+nospZ)_{p1}$	0.03	1 _T	4.5
5	$astar490$	0.02	1 _O	6.9
6	ZQn	0.06	2 _Z	10.63
7	mA	0.05	2 _P	11.21
8	$KG1$	3.96×10^{-3}	2 _{OM}	14.65
9	$astarOMA$	1.47×10^{-3}	2 _O	14.72
Nitrate				
1	$umax$	8.49	1 _P	1
Phosphate				
1	ZKa	1.47	1 _Z	1
2	$umax$	0.78	1 _P	11.45
3	$Tref(nospA+nospZ)_{p1}$	0.16	1 _T	13.71
4	$KG1$	0.14	1 _{OM}	14.64
POM				
1	mA	7.22	1 _P	1
2	$Zumax$	0.96	1 _Z	1.15
3	$KG1$	0.92	1 _{OM}	3.87
4	$Tref(nospA+nospZ)_{p1}$	0.86	1 _T	3.93
5	$astar490$	0.03	1 _O	5.81

Table 6: Results of model calibration to observed O_2 for each of seven parameter subsets selected by sensitivity within each parameter category (first), independent of category (second), and equally within each category (third). The collinearity values (γ) and parameters of each subset are from Tables 3 to 5. Mean L1 is the average of sensitivity values (eq. (2)) for the subset. $RMSE$ shows the final error comparing observed and model output after the specified number of iterations for optimization.

Selection heuristic	γ	n parameters	mean L1	Iterations	$RMSE^*$
1					
Optics	3.87	3	2.81×10^{-4}	133	35.33
Organic Matter	8.61	5	3.18×10^{-3}	231	35.33
Phytoplankton	3.97	7	0.02	180	34.63
Temperature	1	1	0.02	3	35.33
Zooplankton	5.2	4	0.03	117	35.32
2					
Independent of category	6.81	8	0.03	289	35.29
3					
Equally within category	5.22	7	0.03	180	35.32

*Starting $RMSE$ 35.33

Table 7: Results of parameter changes from model calibration to observed O_2 for each of seven parameter subsets selected by sensitivity within each parameter category (first), independent of category (second), and equally within each category (third). The parameters of each subset are from Tables 3 to 5. The L1 values are relative sensitivity of O_2 to a parameter change. Starting and final parameter values after calibration are shown, including the percent change. The calibration routing was bounded by minimum and maximum values appropriate for each parameter.

Selection heuristic	Parameter	L1	Min	Max	Initial	Final	% change
1							
Optics	<i>astar490</i>	7.51×10^{-4}	0.02	0.12	0.04	0.04	-0
	<i>astarOMZ</i>	4.92×10^{-5}	0.01	0.15	0.01	0.01	nc
	<i>astarOMA</i>	4.39×10^{-5}	0.01	0.15	0.01	0.01	nc
Organic Matter	<i>KG1</i>	6.15×10^{-3}	5	100	30	30.02	+0
	<i>KG2</i>	3.14×10^{-3}	5	100	30	30.06	+0
	<i>KstarO2</i>	3.04×10^{-3}	1	100	10	10	nc
	<i>KGcdom</i>	2.98×10^{-3}	0	1	0.01	0.01	nc
	<i>KO2</i>	5.85×10^{-4}	1	100	10	10.18	+2
Phytoplankton	<i>umax</i>	0.05	0.1	2.5	1.12	2.5	+123
	<i>mA</i>	0.02	0.01	0.5	0.11	0.01	-91
	<i>alpha</i>	0.02	1×10^{-17}	6×10^{-16}	3.96×10^{-16}	6×10^{-16}	+52
	<i>ediblevector(Z1)</i>	0.02	0.05	1	0.5	0.5	nc
	<i>Qc</i>	0.01	1×10^{-9}	5×10^{-7}	4.54×10^{-8}	5×10^{-7}	+1001
	<i>respg</i>	8.36×10^{-3}	0.01	0.5	0.1	0.1	nc
	<i>vmaxN</i>	8.12×10^{-3}	1×10^{-11}	1×10^{-8}	1.33×10^{-9}	1.33×10^{-9}	nc
Temperature	<i>Tref(nospA+nospZ)_{p1}</i>	0.02	0	40	17	17	nc
Zooplankton	<i>ZKa</i>	0.05	1×10^{11}	2.5×10^{12}	1.12×10^{12}	1.12×10^{12}	nc
	<i>ZQn</i>	0.02	1×10^{-6}	2.04×10^{-4}	6.95×10^{-5}	6.95×10^{-5}	nc
	<i>Zm</i>	0.02	1×10^{-4}	10	7.2×10^{-4}	6.96×10^{-3}	+867
	<i>Zumax</i>	0.02	5×10^8	2×10^9	9.45×10^8	9.45×10^8	nc
2							
Independent of category	<i>umax</i>	0.05	0.1	2.5	1.12	2.5	+123
	<i>ZKa</i>	0.05	1×10^{11}	2.5×10^{12}	1.12×10^{12}	1.12×10^{12}	nc
	<i>mA</i>	0.02	0.01	0.5	0.11	0.01	-91
	<i>Tref(nospA+nospZ)_{p1}</i>	0.02	0	40	17	17	nc
	<i>ZQn</i>	0.02	1×10^{-6}	2.04×10^{-4}	6.95×10^{-5}	6.95×10^{-5}	nc
	<i>alpha</i>	0.02	1×10^{-17}	6×10^{-16}	3.96×10^{-16}	6×10^{-16}	+52
	<i>Zm</i>	0.02	1×10^{-4}	10	7.2×10^{-4}	5.47×10^{-3}	+660
	<i>Zumax</i>	0.02	5×10^8	2×10^9	9.45×10^8	9.45×10^8	nc
3							
Equally within category	<i>umax</i>	0.05	0.1	2.5	1.12	2.5	+123
	<i>ZKa</i>	0.05	1×10^{11}	2.5×10^{12}	1.12×10^{12}	1.12×10^{12}	nc
	<i>mA</i>	0.02	0.01	0.5	0.11	0.01	-91
	<i>Tref(nospA+nospZ)_{p1}</i>	0.02	0	40	17	17	nc
	<i>ZQn</i>	0.02	1×10^{-6}	2.04×10^{-4}	6.95×10^{-5}	6.95×10^{-5}	nc
	<i>KG1</i>	6.15×10^{-3}	5	100	30	28.11	-6
	<i>astar490</i>	7.51×10^{-4}	0.02	0.12	0.04	0.03	-12

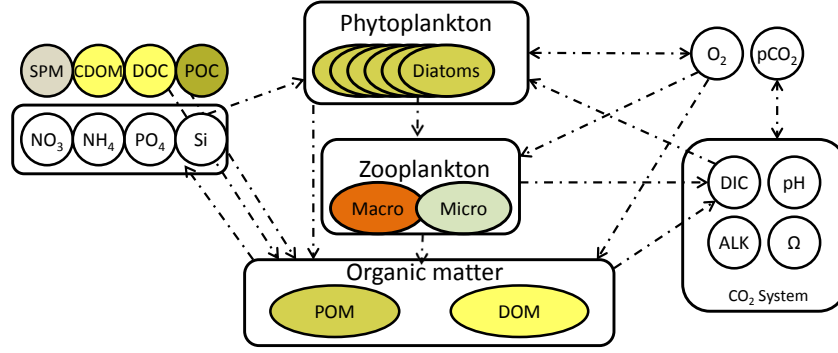


Fig. 1: Conceptual representation of biogeochemical components included in FishTank (complete equations in [Eldridge and Roelke 2010](#)). The Coastal General Ecosystem Model couples FishTank with a hydrodynamic model that includes advection, mixing, and dispersion.

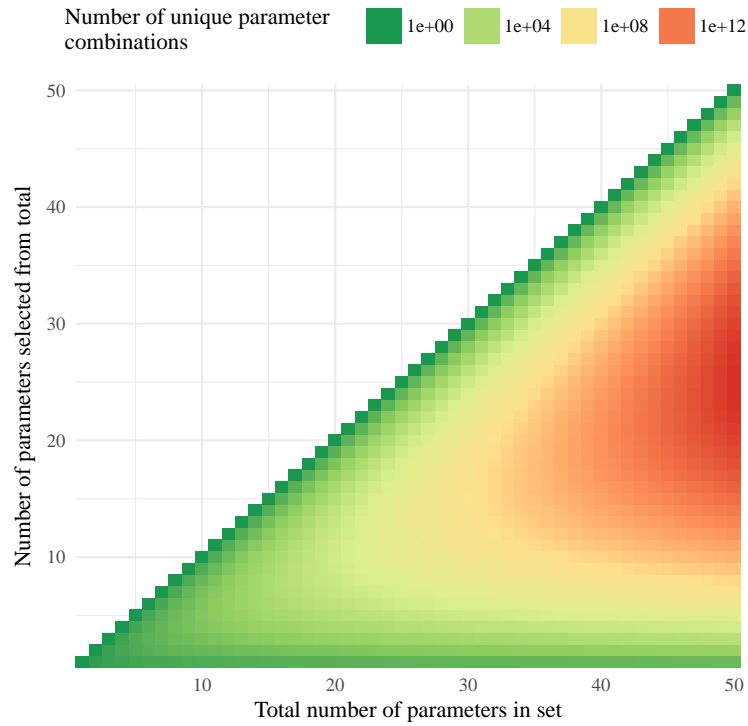


Fig. 2: Examples of unique parameter combinations from different parameter sets and number of selected parameters. The number of combinations are shown for increasing numbers of selected parameters from the total in the set, where 50 parameter sets are shown each with one through 50 total parameters. Note that the number of unique combinations is shown as the natural-log.

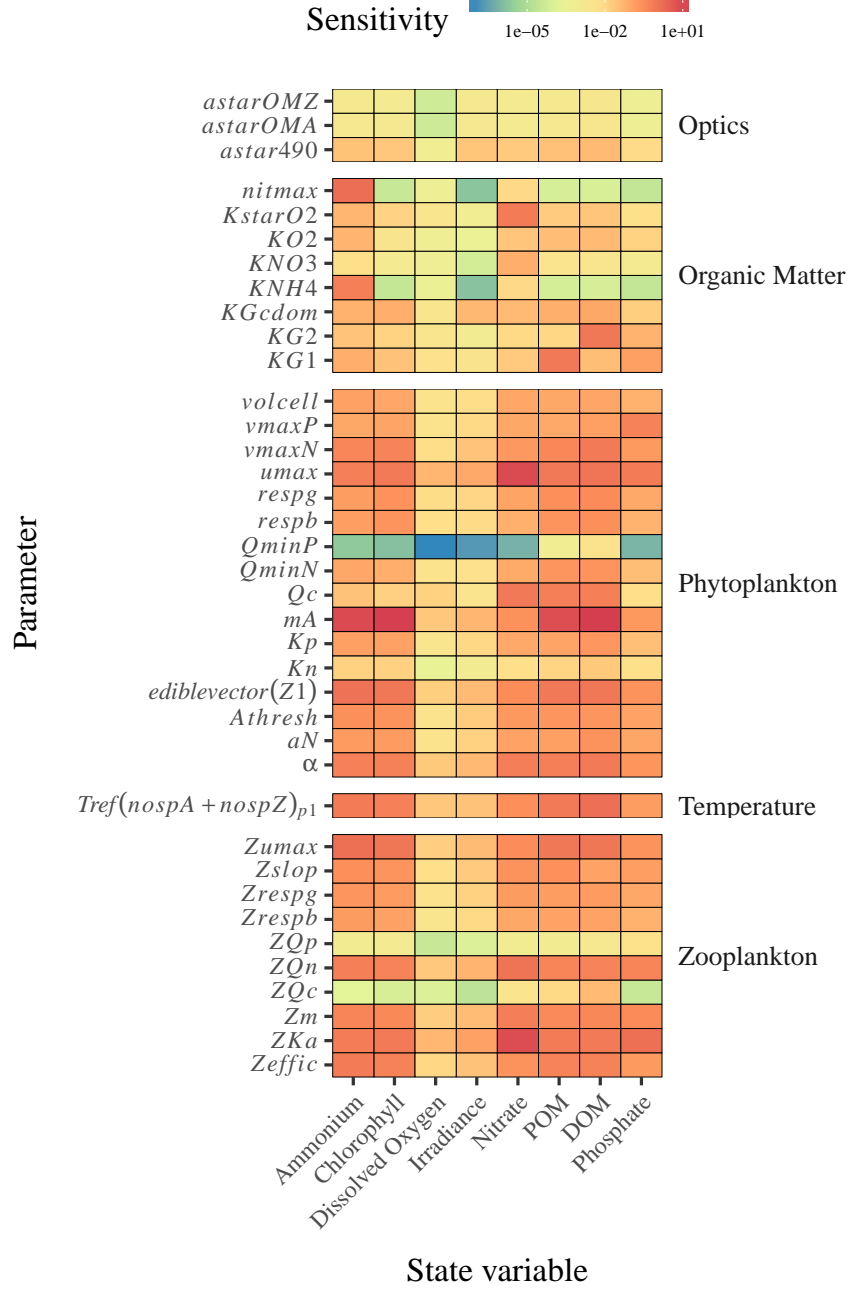


Fig. 3: Sensitivity values (L1, eq. (2)) of all state variables to changes in a 50% increase in parameter values. Parameters are grouped by category: optics, organic matter, phytoplankton, zooplankton, temperature, and zooplankton. See Table 2 for L1 values for O₂ and Tables S1 to S7 for the other state variables.

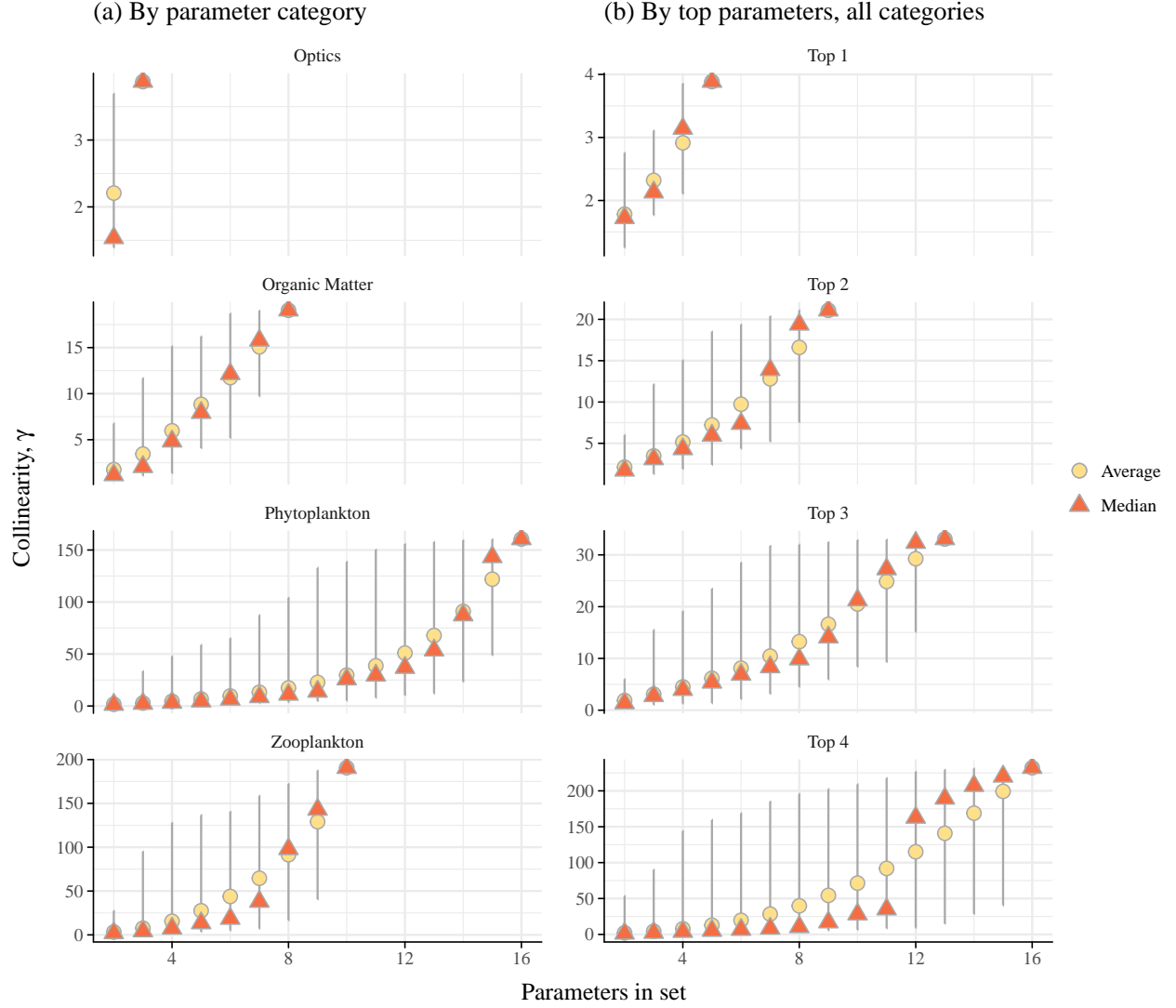


Fig. 4: Collinearity (γ as a measure of identifiability, eq. (3)) of parameter subsets for O_2 . Plots in (a) show collinearity by parameter categories and (b) shows collinearity by selecting the top 1 through 4 parameters in all categories. Lines represent collinearity ranges for the possible combinations given the number of parameters in the set. The temperature category is not shown because O_2 was sensitive to only one parameter (i.e., $\gamma = 1$).

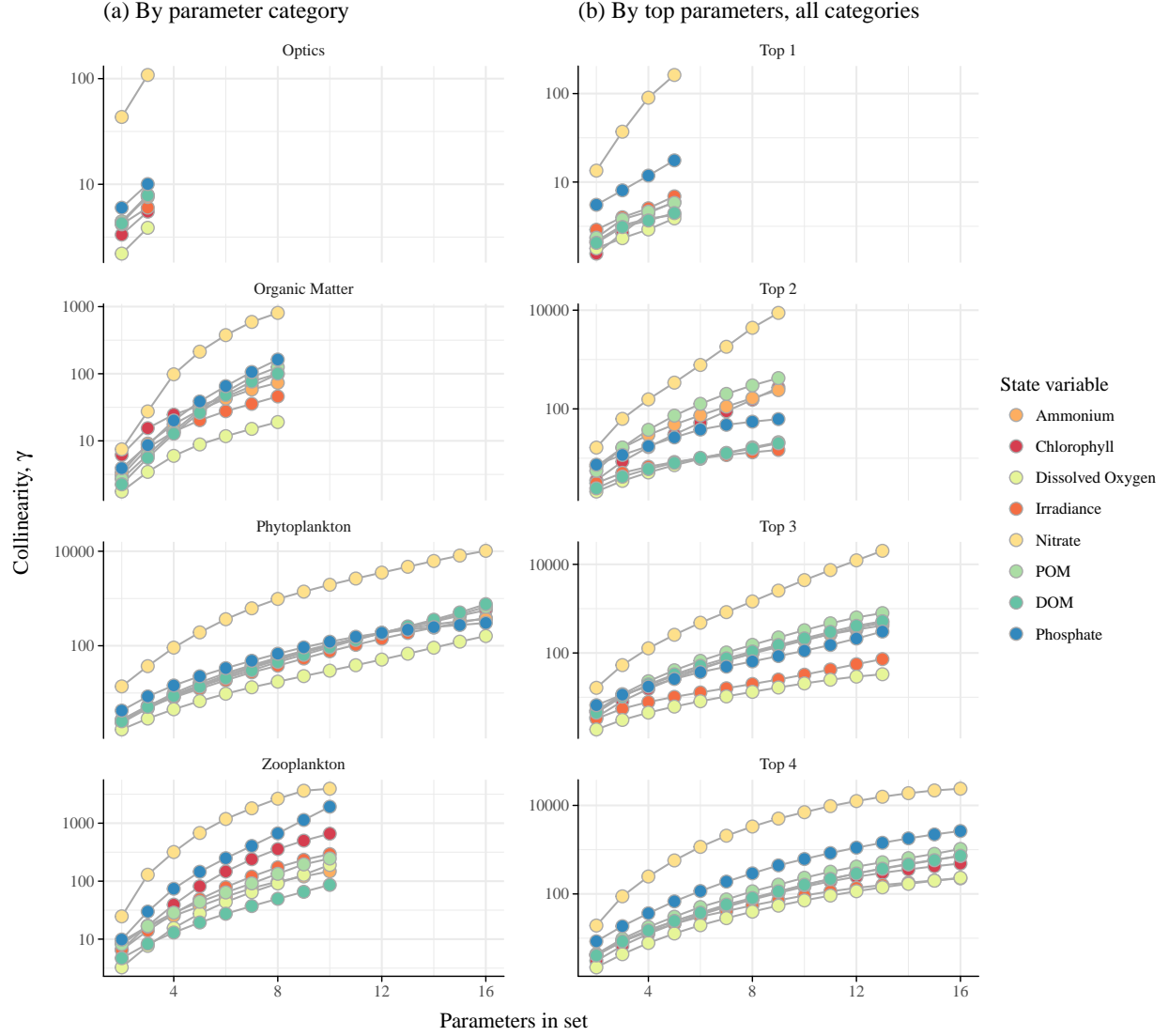


Fig. 5: Average collinearity (γ as a measure of identifiability, eq. (3)) of parameter subsets for all state variables. Plots in (a) show collinearity by parameter categories and (b) shows collinearity by selecting the top 1 through 4 parameters in all categories. Collinearity was averaged for all combinations in a parameter set to evaluate relative differences between state variables. The temperature category is not shown because all state variables were sensitive to only one parameter (i.e., $\gamma = 1$).

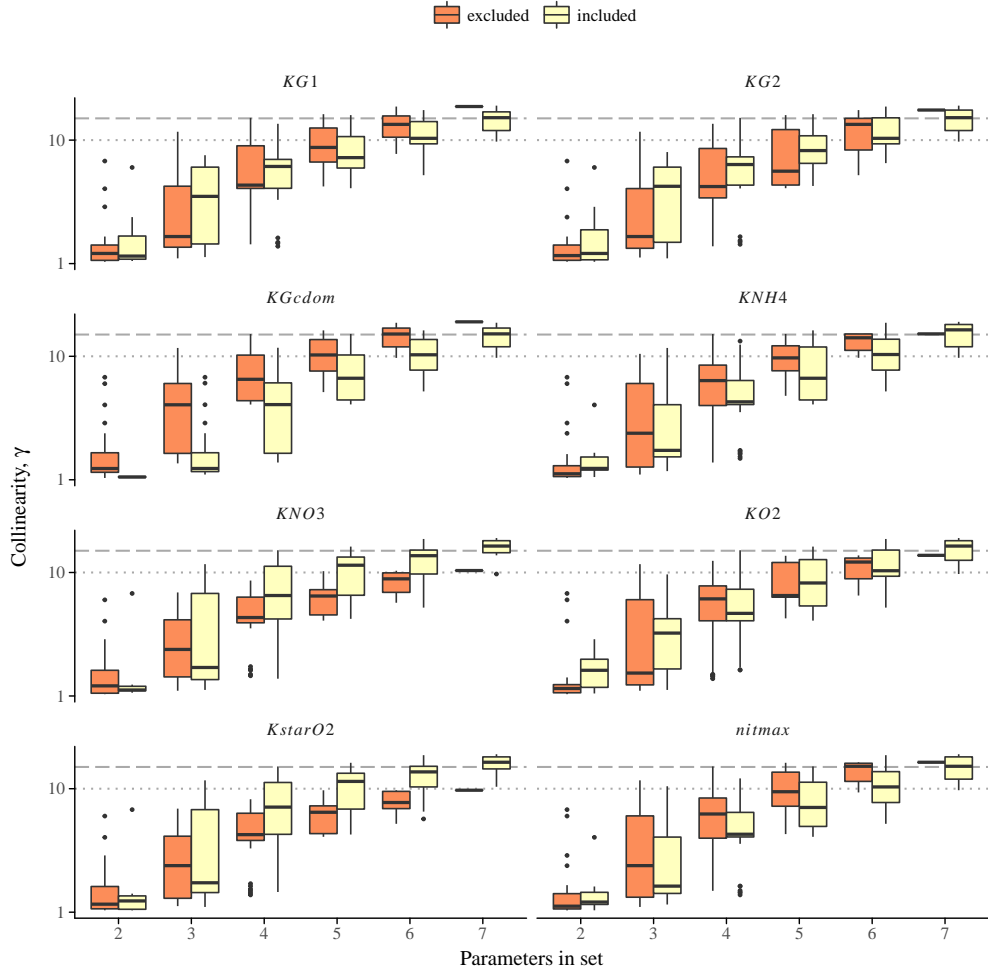


Fig. 6: Collinearity (γ as a measure of identifiability, eq. (3)) for O_2 of organic matter parameters for subset combinations in Fig. 4. Collinearity is evaluated for subsets that excluded and included the parameters at the top of each plot. Collinearity of including all eight parameters is in Fig. 4. Grey lines indicate potential thresholds at $\gamma = 10, 15$ for maximum acceptable collinearity.

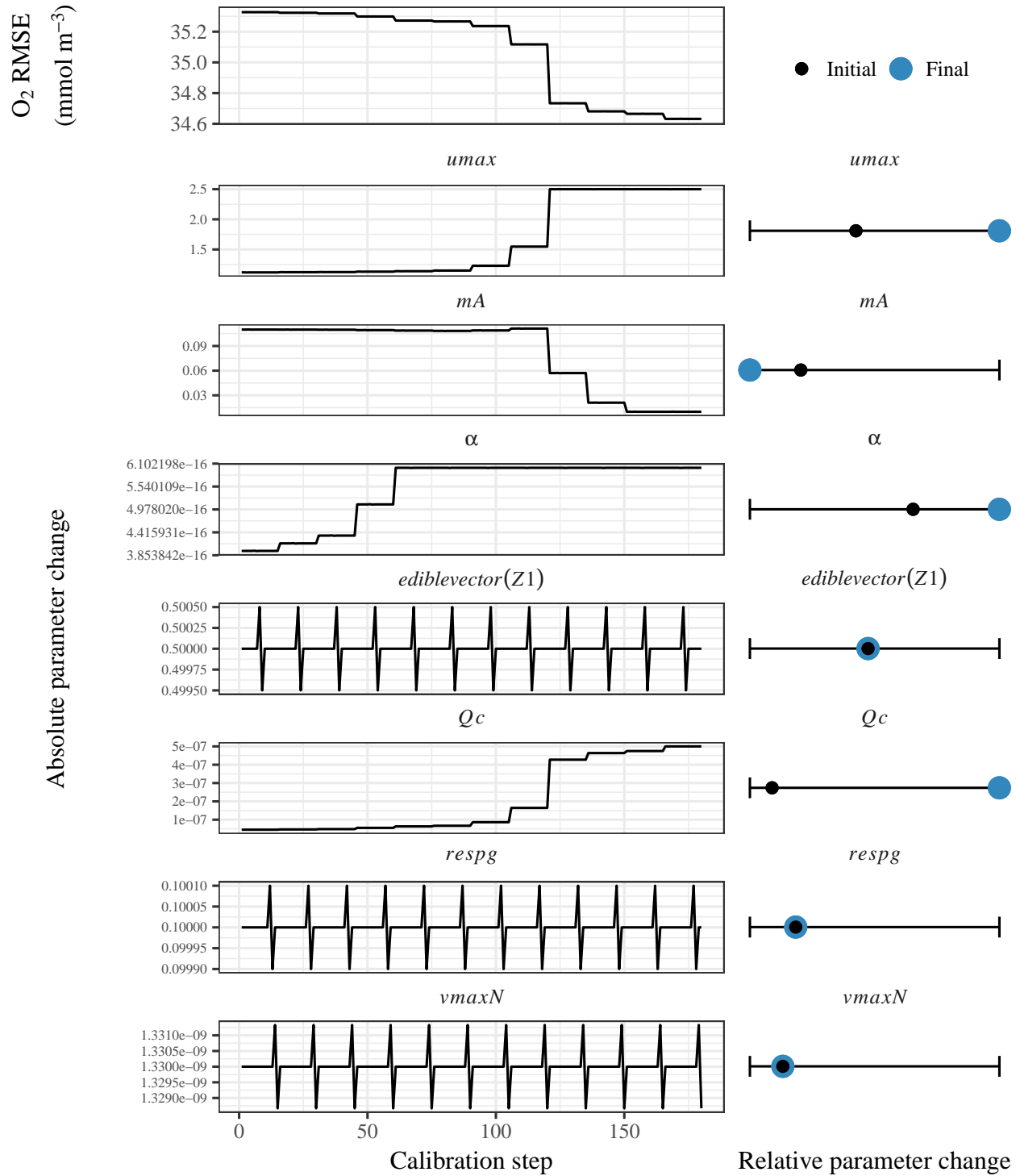


Fig. 7: Example of calibration steps for the phytoplankton parameter subset. The FishTank model was calibrated using data from an approximate 12-hour flask experiment of oxygen production. Model calibration adjusted parameters (left plots) to minimize the *RMSE* between experimental and modelled dissolved oxygen (top left). The phytoplankton parameters were those identifiable for dissolved oxygen (Table 3), arranged from most (top plot) to least sensitive (bottom plot) (Table 2). The relative parameter changes in the right plots show the initial parameter values (black) and the the selected parameter values (blue) after calibration.

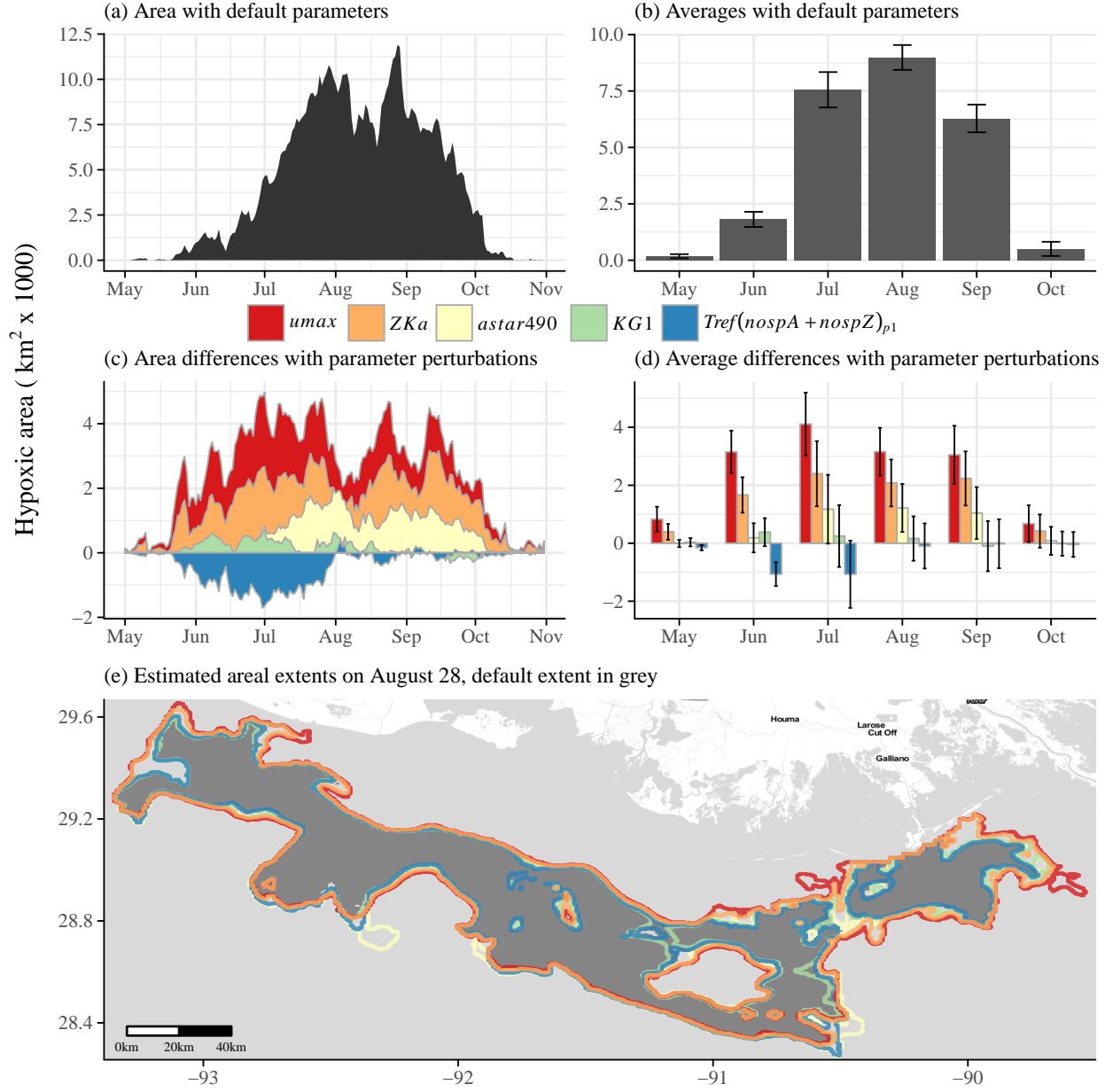


Fig. 8: Estimated hypoxic area and monthly averages (km² × 1000) using the default parameter settings (a, b) and the differences using a 50% increase in each parameter (c, d). The selected parameters were the top sensitive in each parameter category for O₂ in Fig. 3 and Table 2. Error bars are 95% confidence intervals for the monthly averages in (b) and the difference in monthly averages (d) from the perturbed and default results. Areal extent of estimated hypoxia on August 28th using the default parameters (grey) and estimated changes with parameter perturbations is shown in (e).

Table S1: Sensitivity of ammonium to perturbations of individual parameters. Sensitivities are based on a 50% increase from the initial parameter value, where $L1$ summarizes differences in model output (see eq. (2)). Parameters that did not affect ammonium are not shown. Parameters are grouped by categories as optics, temperature, phytoplankton, zooplankton, and organic matter.

Description	Parameter	L1
Optics		
Chla specific absorption at 490 nm	<i>astar490</i>	0.03
OMA specific absorption at 490 nm	<i>astarOMA</i>	1.63×10^{-3}
OMZ specific absorption at 490 nm	<i>astarOMZ</i>	1.5×10^{-3}
Organic Matter		
maximum rate of nitrification per day	<i>nitmax</i>	1.54
NH4 rate constant for nitrification	<i>KNH4</i>	0.66
turnover rate for OM1A and OM1Z	<i>KG1</i>	0.07
decay rate of CDOM	<i>KGcdom</i>	0.07
half-saturation concentration for O2 utilization	<i>KO2</i>	0.06
O2 concentration that inhibits denitrification	<i>KstarO2</i>	0.05
turnover rate for OM2A and OM2Z	<i>KG2</i>	0.03
half-saturation concentration for denitrification	<i>KNO3</i>	7.55×10^{-3}
Phytoplankton		
mortality coefficient	<i>mA</i>	8.49
edibility vector for Z1	<i>ediblevector(Z1)</i>	1.32
maximum growth rate	<i>umax</i>	0.65
initial slope of photosynthesis v irradiance	<i>alpha</i>	0.6
N-uptake rate measured at umax	<i>vmaxN</i>	0.46
phytoplankton threshold for grazing	<i>Athresh</i>	0.29
coefficient for non-limiting nutrient	<i>aN</i>	0.17
phytoplankton growth respiration coefficient	<i>respg</i>	0.16
phytoplankton basal respiration coefficient	<i>respb</i>	0.15
half-saturation constant for P	<i>Kp</i>	0.14
phytoplankton volume/cell	<i>volcell</i>	0.14
minimum N cell-quota	<i>QminN</i>	0.1
P-uptake rate measured at umax	<i>vmaxP</i>	0.1
phytoplankton carbon/cell	<i>Qc</i>	0.03
half-saturation constant for N	<i>Kn</i>	0.01
minimum P cell-quota	<i>QminP</i>	2.24×10^{-6}
Temperature		
Optimum temperature for growth	<i>Tref(nospA+nospZ)_{p1}</i>	0.79
Zooplankton		
maximum growth rate of zooplankton	<i>Zumax</i>	1.42
assimilation efficiency as a fraction of ingestion	<i>Zeffic</i>	0.76
half saturation coefficient for grazing	<i>ZKa</i>	0.74
zooplankton nitrogen/individual	<i>ZQn</i>	0.62
quadratic mortality constant	<i>Zm</i>	0.5
proportion of phytoplankton lost to sloppy feeding	<i>Zslop</i>	0.3
zooplankton growth-dependent respiration factor	<i>Zrespg</i>	0.22
zooplankton biomass-dependent respiration factor	<i>Zrespb</i>	0.16
zooplankton phosphorus/individual	<i>ZQp</i>	1.07×10^{-3}
zooplankton carbon/individual	<i>ZQc</i>	1.44×10^{-4}

Table S2: Sensitivity of chl-*a* to perturbations of individual parameters. Sensitivities are based on a 50% increase from the initial parameter value, where *L1* summarizes differences in model output (see eq. (2)). Parameters that did not affect chl-*a* are not shown. Parameters are grouped by categories as optics, temperature, phytoplankton, zooplankton, and organic matter.

Description	Parameter	L1
Optics		
Chla specific absorption at 490 nm	<i>astar490</i>	0.02
OMA specific absorption at 490 nm	<i>astarOMA</i>	1.45×10^{-3}
OMZ specific absorption at 490 nm	<i>astarOMZ</i>	1.13×10^{-3}
Organic Matter		
decay rate of CDOM	<i>KGcdom</i>	0.07
turnover rate for OM1A and OM1Z	<i>KG1</i>	0.03
turnover rate for OM2A and OM2Z	<i>KG2</i>	0.01
O2 concentration that inhibits denitrification	<i>KstarO2</i>	0.01
half-saturation concentration for O2 utilization	<i>KO2</i>	3.35×10^{-3}
half-saturation concentration for denitrification	<i>KNO3</i>	1.19×10^{-3}
maximum rate of nitrification per day	<i>nitmax</i>	3.4×10^{-5}
NH4 rate constant for nitrification	<i>KNH4</i>	2.97×10^{-5}
Phytoplankton		
mortality coefficient	<i>mA</i>	13.94
edibility vector for Z1	<i>ediblevector(Z1)</i>	0.95
maximum growth rate	<i>umax</i>	0.85
initial slope of photosynthesis v irradiance	<i>alpha</i>	0.62
N-uptake rate measured at umax	<i>vmaxN</i>	0.53
phytoplankton growth respiration coefficient	<i>respg</i>	0.26
phytoplankton threshold for grazing	<i>Athresh</i>	0.25
phytoplankton basal respiration coefficient	<i>respb</i>	0.24
coefficient for non-limiting nutrient	<i>aN</i>	0.17
half-saturation constant for P	<i>Kp</i>	0.14
P-uptake rate measured at umax	<i>vmaxP</i>	0.12
phytoplankton volume/cell	<i>volcell</i>	0.1
minimum N cell-quota	<i>QminN</i>	0.07
phytoplankton carbon/cell	<i>Qc</i>	0.02
half-saturation constant for N	<i>Kn</i>	0.01
minimum P cell-quota	<i>QminP</i>	1.38×10^{-6}
Temperature		
Optimum temperature for growth	<i>Tref(nospA+nospZ)_{p1}</i>	0.6
Zooplankton		
maximum growth rate of zooplankton	<i>Zumax</i>	1.02
half saturation coefficient for grazing	<i>ZKa</i>	0.85
assimilation efficiency as a fraction of ingestion	<i>Zeffic</i>	0.57
zooplankton nitrogen/individual	<i>ZQn</i>	0.52
quadratic mortality constant	<i>Zm</i>	0.41
proportion of phytoplankton lost to sloppy feeding	<i>Zslop</i>	0.23
zooplankton growth-dependent respiration factor	<i>Zrespg</i>	0.17
zooplankton biomass-dependent respiration factor	<i>Zrespb</i>	0.14
zooplankton phosphorus/individual	<i>ZQp</i>	1.29×10^{-3}
zooplankton carbon/individual	<i>ZQc</i>	7.55×10^{-5}

Table S3: Sensitivity of irradiance to perturbations of individual parameters. Sensitivities are based on a 50% increase from the initial parameter value, where $L1$ summarizes differences in model output (see eq. (2)). Parameters that did not affect irradiance are not shown. Parameters are grouped by categories as optics, temperature, phytoplankton, zooplankton, and organic matter.

Description	Parameter	L1
Optics		
Chla specific absorption at 490 nm	$astar_{490}$	0.02
OMA specific absorption at 490 nm	$astar_{OMA}$	1.47×10^{-3}
OMZ specific absorption at 490 nm	$astar_{OMZ}$	1.34×10^{-3}
Organic Matter		
decay rate of CDOM	KG_{cdom}	0.05
turnover rate for OM1A and OM1Z	$KG1$	3.96×10^{-3}
turnover rate for OM2A and OM2Z	$KG2$	9.88×10^{-4}
O2 concentration that inhibits denitrification	$Kstar_{O2}$	7.2×10^{-4}
half-saturation concentration for O2 utilization	$KO2$	3.54×10^{-4}
half-saturation concentration for denitrification	$KNO3$	6.18×10^{-5}
maximum rate of nitrification per day	$nitmax$	1.72×10^{-6}
NH4 rate constant for nitrification	KNH_4	1.48×10^{-6}
Phytoplankton		
maximum growth rate	$umax$	0.09
mortality coefficient	mA	0.05
initial slope of photosynthesis v irradiance	$alpha$	0.04
edibility vector for Z1	$ediblevector(Z1)$	0.04
N-uptake rate measured at umax	$vmaxN$	0.03
phytoplankton threshold for grazing	$Athresh$	0.02
coefficient for non-limiting nutrient	aN	0.01
phytoplankton growth respiration coefficient	$respg$	0.01
half-saturation constant for P	Kp	0.01
P-uptake rate measured at umax	$vmaxP$	9.48×10^{-3}
phytoplankton basal respiration coefficient	$respb$	9.38×10^{-3}
phytoplankton volume/cell	$volcell$	8.1×10^{-3}
minimum N cell-quota	$QminN$	5.75×10^{-3}
phytoplankton carbon/cell	Qc	3.78×10^{-3}
half-saturation constant for N	Kn	9.81×10^{-4}
minimum P cell-quota	$QminP$	1.92×10^{-7}
Temperature		
Optimum temperature for growth	$Tref(nospA+nospZ)_{p1}$	0.03
Zooplankton		
half saturation coefficient for grazing	ZKa	0.13
zooplankton nitrogen/individual	ZQn	0.06
maximum growth rate of zooplankton	$Zumax$	0.04
quadratic mortality constant	Zm	0.04
assimilation efficiency as a fraction of ingestion	$Zeffic$	0.03
proportion of phytoplankton lost to sloppy feeding	$Zslop$	0.02
zooplankton growth-dependent respiration factor	$Zrespg$	0.01
zooplankton biomass-dependent respiration factor	$Zrespb$	9.67×10^{-3}
zooplankton phosphorus/individual	ZQp	9.34×10^{-5}
zooplankton carbon/individual	ZQc	1.99×10^{-5}

Table S4: Sensitivity of nitrate to perturbations of individual parameters. Sensitivities are based on a 50% increase from the initial parameter value, where $L1$ summarizes differences in model output (see eq. (2)). Parameters that did not affect nitrate are not shown. Parameters are grouped by categories as optics, temperature, phytoplankton, zooplankton, and organic matter.

Description	Parameter	L1
Optics		
Chla specific absorption at 490 nm	$astar_{490}$	0.02
OMZ specific absorption at 490 nm	$astar_{OMZ}$	1.27×10^{-3}
OMA specific absorption at 490 nm	$astar_{OMA}$	1.19×10^{-3}
Organic Matter		
O2 concentration that inhibits denitrification	$Kstar_{O2}$	0.78
half-saturation concentration for denitrification	$KNO3$	0.07
decay rate of CDOM	KG_{cdom}	0.04
half-saturation concentration for O2 utilization	$KO2$	0.03
turnover rate for OM1A and OM1Z	$KG1$	0.02
turnover rate for OM2A and OM2Z	$KG2$	0.01
maximum rate of nitrification per day	$nitmax$	9.96×10^{-3}
NH4 rate constant for nitrification	KNH_4	9.87×10^{-3}
Phytoplankton		
maximum growth rate	$umax$	8.49
phytoplankton carbon/cell	Qc	0.89
initial slope of photosynthesis v irradiance	$alpha$	0.7
edibility vector for Z1	$ediblevector(Z1)$	0.33
mortality coefficient	mA	0.27
phytoplankton threshold for grazing	$Athresh$	0.2
N-uptake rate measured at umax	$vmaxN$	0.19
coefficient for non-limiting nutrient	aN	0.13
phytoplankton growth respiration coefficient	$respg$	0.11
phytoplankton volume/cell	$volcell$	0.1
P-uptake rate measured at umax	$vmaxP$	0.1
half-saturation constant for P	Kp	0.09
minimum N cell-quota	$QminN$	0.09
phytoplankton basal respiration coefficient	$respb$	0.07
half-saturation constant for N	Kn	7.06×10^{-3}
minimum P cell-quota	$QminP$	6.67×10^{-7}
Temperature		
Optimum temperature for growth	$Tref(nospA + nospZ)_{p1}$	0.3
Zooplankton		
half saturation coefficient for grazing	ZKa	7.59
zooplankton nitrogen/individual	ZQn	1.17
quadratic mortality constant	Zm	0.7
maximum growth rate of zooplankton	$Zumax$	0.34
proportion of phytoplankton lost to sloppy feeding	$Zslop$	0.26
assimilation efficiency as a fraction of ingestion	$Zeffic$	0.25
zooplankton growth-dependent respiration factor	$Zrespg$	0.17
zooplankton biomass-dependent respiration factor	$Zrespb$	0.1
zooplankton carbon/individual	ZQc	3.8×10^{-3}
zooplankton phosphorus/individual	ZQp	8.59×10^{-4}

Table S5: Sensitivity of POM to perturbations of individual parameters. Sensitivities are based on a 50% increase from the initial parameter value, where $L1$ summarizes differences in model output (see eq. (2)). Parameters that did not affect POM are not shown. Parameters are grouped by categories as optics, temperature, phytoplankton, zooplankton, and organic matter.

Description	Parameter	L1
Optics		
Chla specific absorption at 490 nm	$astar_{490}$	0.03
OMA specific absorption at 490 nm	$astar_{OMA}$	1.73×10^{-3}
OMZ specific absorption at 490 nm	$astar_{OMZ}$	1.49×10^{-3}
Organic Matter		
turnover rate for OM1A and OM1Z	$KG1$	0.92
decay rate of CDOM	KG_{cdom}	0.07
half-saturation concentration for O2 utilization	$KO2$	0.04
O2 concentration that inhibits denitrification	$KstarO2$	0.02
turnover rate for OM2A and OM2Z	$KG2$	0.01
half-saturation concentration for denitrification	$KNO3$	3.72×10^{-3}
maximum rate of nitrification per day	$nitmax$	6.98×10^{-5}
NH4 rate constant for nitrification	KNH_4	6.41×10^{-5}
Phytoplankton		
mortality coefficient	mA	7.22
edibility vector for Z1	$ediblevector(Z1)$	0.9
maximum growth rate	$umax$	0.89
phytoplankton carbon/cell	Qc	0.67
initial slope of photosynthesis v irradiance	$alpha$	0.67
N-uptake rate measured at umax	$vmaxN$	0.45
phytoplankton growth respiration coefficient	$respg$	0.29
phytoplankton basal respiration coefficient	$respb$	0.24
phytoplankton threshold for grazing	$Athresh$	0.22
minimum N cell-quota	$QminN$	0.21
coefficient for non-limiting nutrient	aN	0.14
half-saturation constant for P	Kp	0.11
phytoplankton volume/cell	$volcell$	0.1
P-uptake rate measured at umax	$vmaxP$	0.09
half-saturation constant for N	Kn	0.01
minimum P cell-quota	$QminP$	7.35×10^{-4}
Temperature		
Optimum temperature for growth	$Tref(nospA + nospZ)_{p1}$	0.86
Zooplankton		
maximum growth rate of zooplankton	$Zumax$	0.96
half saturation coefficient for grazing	ZKa	0.79
assimilation efficiency as a fraction of ingestion	$Zeffc$	0.54
zooplankton nitrogen/individual	ZQn	0.49
quadratic mortality constant	Zm	0.39
proportion of phytoplankton lost to sloppy feeding	$Zslop$	0.27
zooplankton growth-dependent respiration factor	$Zrespg$	0.16
zooplankton biomass-dependent respiration factor	$Zrespb$	0.12
zooplankton carbon/individual	ZQc	9.64×10^{-3}
zooplankton phosphorus/individual	ZQp	1.06×10^{-3}

Table S6: Sensitivity of dissolved organic matter to perturbations of individual parameters. Sensitivities are based on a 50% increase from the initial parameter value, where $L1$ summarizes differences in model output (see eq. (2)). Parameters that did not affect dissolved organic matter are not shown. Parameters are grouped by categories as optics, temperature, phytoplankton, zooplankton, and organic matter.

Description	Parameter	L1
Optics		
Chla specific absorption at 490 nm	$astar_{490}$	0.04
OMA specific absorption at 490 nm	$astar_{OMA}$	2.48×10^{-3}
OMZ specific absorption at 490 nm	$astar_{OMZ}$	2.04×10^{-3}
Organic Matter		
turnover rate for OM2A and OM2Z	$KG2$	0.94
decay rate of CDOM	KG_{cdom}	0.1
half-saturation concentration for O2 utilization	$KO2$	0.04
turnover rate for OM1A and OM1Z	$KG1$	0.04
O2 concentration that inhibits denitrification	$KstarO2$	0.03
half-saturation concentration for denitrification	$KNO3$	3.16×10^{-3}
maximum rate of nitrification per day	$nitmax$	8.44×10^{-5}
NH4 rate constant for nitrification	KNH_4	7.41×10^{-5}
Phytoplankton		
mortality coefficient	mA	14.25
maximum growth rate	$umax$	1.11
edibility vector for Z1	$ediblevector(Z1)$	0.94
N-uptake rate measured at umax	$vmaxN$	0.86
initial slope of photosynthesis v irradiance	$alpha$	0.85
phytoplankton carbon/cell	Qc	0.67
phytoplankton growth respiration coefficient	$respg$	0.36
phytoplankton basal respiration coefficient	$respb$	0.29
coefficient for non-limiting nutrient	aN	0.25
minimum N cell-quota	$QminN$	0.24
phytoplankton threshold for grazing	$Athresh$	0.22
half-saturation constant for P	Kp	0.2
P-uptake rate measured at umax	$vmaxP$	0.14
phytoplankton volume/cell	$volcell$	0.1
half-saturation constant for N	Kn	0.02
minimum P cell-quota	$QminP$	4.37×10^{-3}
Temperature		
Optimum temperature for growth	$Tref(nospA+nospZ)_{p1}$	1.48
Zooplankton		
maximum growth rate of zooplankton	$Zumax$	1.01
half saturation coefficient for grazing	ZKa	0.88
assimilation efficiency as a fraction of ingestion	$Zeffic$	0.58
zooplankton nitrogen/individual	ZQn	0.54
quadratic mortality constant	Zm	0.41
zooplankton growth-dependent respiration factor	$Zrespg$	0.17
zooplankton biomass-dependent respiration factor	$Zrespb$	0.13
proportion of phytoplankton lost to sloppy feeding	$Zslop$	0.12
zooplankton carbon/individual	ZQc	0.04
zooplankton phosphorus/individual	ZQp	1.69×10^{-3}

Table S7: Sensitivity of phosphate to perturbations of individual parameters. Sensitivities are based on a 50% increase from the initial parameter value, where $L1$ summarizes differences in model output (see eq. (2)). Parameters that did not affect phosphate are not shown. Parameters are grouped by categories as optics, temperature, phytoplankton, zooplankton, and organic matter.

Description	Parameter	L1
Optics		
Chla specific absorption at 490 nm	<i>astar₄₉₀</i>	9.01×10^{-3}
OMZ specific absorption at 490 nm	<i>astar_{OMZ}</i>	5.21×10^{-4}
OMA specific absorption at 490 nm	<i>astar_{OMA}</i>	5.13×10^{-4}
Organic Matter		
turnover rate for OM1A and OM1Z	<i>KG1</i>	0.14
turnover rate for OM2A and OM2Z	<i>KG2</i>	0.06
decay rate of CDOM	<i>KG_{cdom}</i>	0.02
half-saturation concentration for O2 utilization	<i>KO2</i>	0.01
O2 concentration that inhibits denitrification	<i>KstarO2</i>	7.29×10^{-3}
half-saturation concentration for denitrification	<i>KNO3</i>	1.19×10^{-3}
maximum rate of nitrification per day	<i>nitmax</i>	2.7×10^{-5}
NH4 rate constant for nitrification	<i>KNH₄</i>	2.64×10^{-5}
Phytoplankton		
maximum growth rate	<i>umax</i>	0.78
P-uptake rate measured at umax	<i>vmaxP</i>	0.59
edibility vector for Z1	<i>ediblevector(Z1)</i>	0.25
initial slope of photosynthesis v irradiance	<i>alpha</i>	0.23
mortality coefficient	<i>mA</i>	0.2
N-uptake rate measured at umax	<i>vmaxN</i>	0.18
phytoplankton threshold for grazing	<i>Athresh</i>	0.13
coefficient for non-limiting nutrient	<i>aN</i>	0.11
phytoplankton growth respiration coefficient	<i>respg</i>	0.09
phytoplankton volume/cell	<i>volcell</i>	0.06
phytoplankton basal respiration coefficient	<i>respb</i>	0.06
minimum N cell-quota	<i>QminN</i>	0.04
half-saturation constant for P	<i>Kp</i>	0.03
half-saturation constant for N	<i>Kn</i>	6.97×10^{-3}
phytoplankton carbon/cell	<i>Qc</i>	6.68×10^{-3}
minimum P cell-quota	<i>QminP</i>	8.21×10^{-7}
Temperature		
Optimum temperature for growth	<i>Tref(nospA+nospZ)_{p1}</i>	0.16
Zooplankton		
half saturation coefficient for grazing	<i>ZKa</i>	1.47
zooplankton nitrogen/individual	<i>ZQn</i>	0.5
quadratic mortality constant	<i>Zm</i>	0.35
maximum growth rate of zooplankton	<i>Zumax</i>	0.26
assimilation efficiency as a fraction of ingestion	<i>Zeffic</i>	0.19
proportion of phytoplankton lost to sloppy feeding	<i>Zslop</i>	0.15
zooplankton growth-dependent respiration factor	<i>Zrespg</i>	0.1
zooplankton biomass-dependent respiration factor	<i>Zrespb</i>	0.06
zooplankton phosphorus/individual	<i>ZQp</i>	6.43×10^{-3}
zooplankton carbon/individual	<i>ZQc</i>	3.38×10^{-5}